2370-9

School and Training Course on Dense Magnetized Plasma as a Source of Ionizing Radiations, their Diagnostics and Applications

8 - 12 October 2012

Plasma Focus Numerical Experiments - Scaling Properties to Scaling Laws

S. Lee
INTI International University, 71800 Nilai
Malaysia

Institute for Plasma Focus Studies, Chadstone, VIC 3148
Australia

University of Malaya, Kuala Lumpur
Malaysia

School and Training Course on Dense Magnetized Plasma as a Source of Ionizing Radiations, their Diagnostics and Applications
8-12 October 2012, ICTP, Trieste

Plasma Focus Numerical Experiments- Scaling Properties to Scaling Laws

S Lee[1,2,3] & S H Saw[1,2]

INTI International University, 71800 Nilai, Malaysia

Institute for Plasma Focus Studies, Chadstone, VIC 3148, Australia

University of Malaya, Kuala Lumpur, Malaysia

e-mail: leesing@optusnet.com.au sorheoh.saw@newinti.edu.my

Our Modelling

- Experimental based
- Utility prioritised
- To cover the whole process- from lift-off, to axial, to all the radial sub-phases; and recently to post-focussed phase which is important for advanced materials deposition and damage simulation

Priority of **Basis**

- **Energy** consistent for the total process and each part of the process
- **Mass** consistent
- **Charge** consistent
- Connected to the **reality** of experiments

Priority of **Results**

- **Applicable to all Mather-type PF machines, existing and hypothetical**
- **Current Waveform accuracy**
- **Dynamics in agreement with experiments**
- **Consistency of Energy distribution**
- **Realistic Yields of neutrons, SXR, other radiations; Ions and Plasma Stream; in conformity with experiments**
- **Widest Scaling of the yields; all gases**
- **Insightful definition of scaling properties**
- **Design of new devices; e.g. High V & Current-Step**
- **Design of new experiments; radiative cooling and collapse**

Basis, modelling, results and applications of the Model code

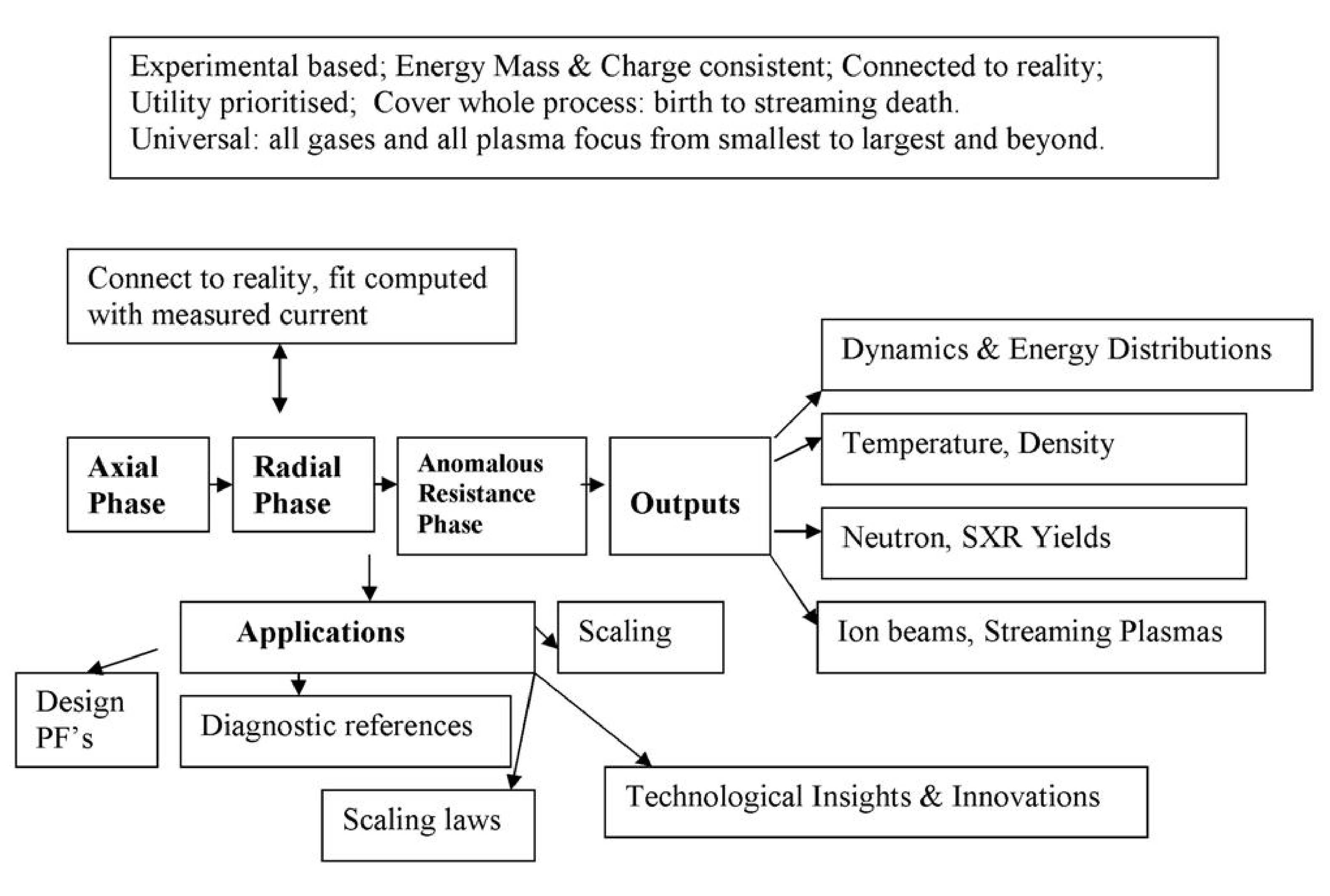

Numerical Experiments

- Range of activities using the code is wide
- Not theoretical
- Not simulation
- The preferred description is:

  Numerical Experiments

Plasma Focus Numerical Experiments-
Scaling Properties & Scaling Laws

Outline of talk:

- Numerical experiments are used to deduce scaling properties of the PF.
- Numerical experiments are used to deduce scaling laws for neutrons and neon SXR.
- We connect the scaling laws as a development from the scaling properties.
- A Global Scaling Law for neutron yields as a function of storage energies is derived from numerical experiments combined with measured data showing a deterioration of scaling due to the dynamic resistance of the axial phase.
- **A by-product of the numerical experiments are diagnostic reference points**.

The Model code-
Comprehensive Numerical Experiments

- To model the plasma dynamics & plasma conditions
- Then obtain insights into scaling properties
- Then scaling laws

Critical to the approach:

Model is linked to physical reality by the current waveform

The Plasma Focus 1/2

- Plasma focus: small fusion device, complements international efforts to build fusion reactor
- Multi-radiation device - x-rays, particle beams and fusion neutrons
- Neutrons for fusion studies
- Soft XR applications include microelectronics lithography and micro-machining
- Large range of device-from J to thousands of kJ
- Experiments-dynamics, radiation, instabilities and non-linear phenomena

The Plasma Focus 2/2

Axial Phase Radial Phases

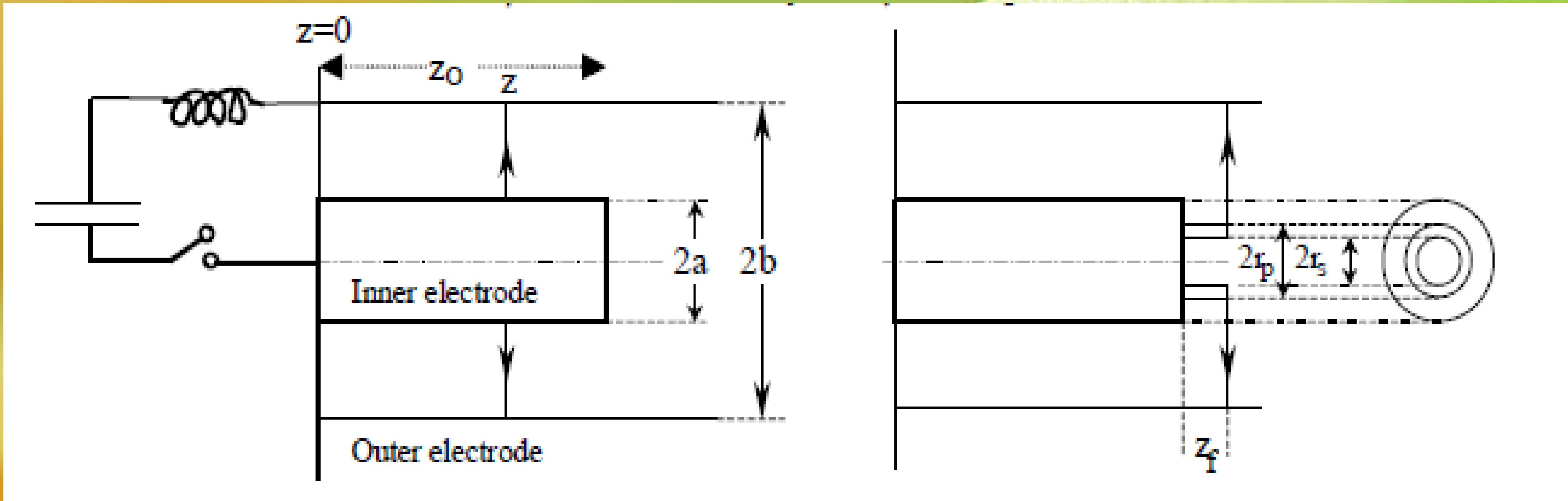

The 5-phases of the Model code

Includes electrodynamical- and radiation- coupled equations to portray the REGULAR mechanisms of the:

- axial (phase 1)
- radial inward shock (phase 2)
- radial RS (phase 3)
- slow compression radiation phase (phase 4)
- the expanded axial post-pinch phase (phase 5)

Crucial technique of the code: Current Fitting

The Model

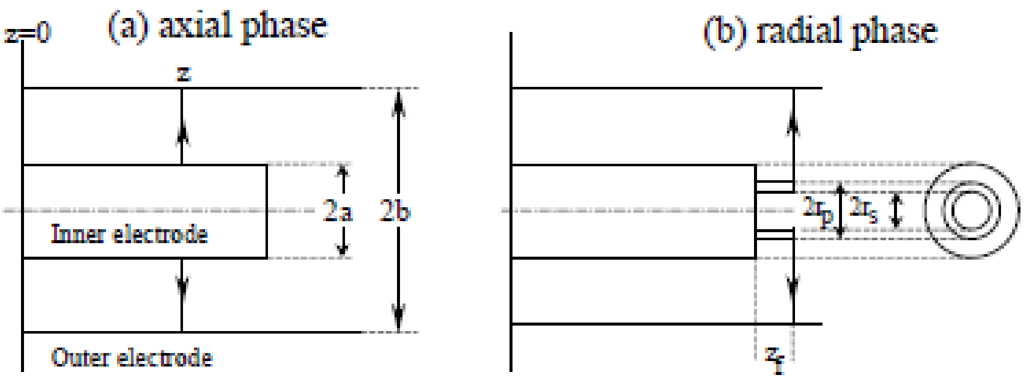

Fig 1: Schematic of (a) axial phase and (b) radial phase /2/

The equations for the axial and radial phases are written and normalised in the following manner [2-4,7]: (geometrical quantities are shown in the Figs 1 & 2, L_o, C_o, r_o are the circuit inductance, capacitance and resistance, V_o is the voltage C_o is charged to).

$$\tau = \frac{t}{t_o},\quad \zeta = \frac{z}{z_o},\quad \iota = \frac{I}{I_o},\quad \delta = \frac{r_o}{Z_o}$$

$$\kappa_s = \frac{r_s}{a},\quad \kappa_p = \frac{r_p}{a},\quad \zeta_f = \frac{z_f}{a}, Z_o = \sqrt{\frac{L_o}{C_o}}$$

$$t_o = \sqrt{L_o C_o} \text{ and } I_o = V_o / Z_o$$

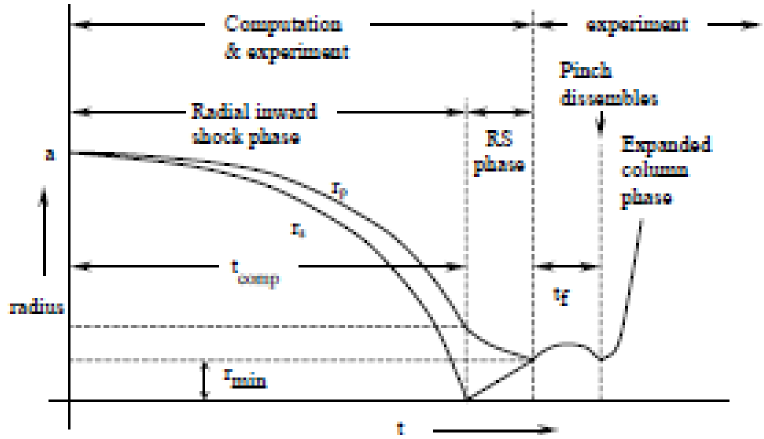

Fig 2. Schematic of radial phases

The Axial Phase- two coupled equations (1) & (2)

Motion: $$\frac{d^2\zeta}{d\tau^2} = \frac{\alpha^2\iota^2 - \left(\frac{d\zeta}{d\tau}\right)^2}{\zeta} \tag{1}$$

Current: $$\frac{d\iota}{d\tau} = \frac{1 - \int \iota\, d\tau - f_c\beta \frac{d\zeta}{d\tau}\iota - \delta\iota}{1 + f_c\beta\zeta} \tag{2}$$

to compute ϕ and ι; with two scaling parameters:

$$\beta = \left[\frac{\mu}{2\pi} z_o \ln c\right] / L_o \tag{3}$$

which is the ratio of the full axial phase tube inductance to the external fixed inductance. Ratio of characteristic electrical discharge time to characteristic axial transit times is:

$$\alpha = t_a / t_s \tag{4}$$

$$\text{where} \quad t_a = \left[\frac{4\pi^2(c^2-1)}{\mu \ln c}\right]^{1/2} \frac{z_o\sqrt{f_m}}{f_c} \frac{\sqrt{\rho}}{(I_o/a)} \tag{5}$$

The characteristic speed and The **Speed Factor**

giving a characteristic axial transit speed of $v_a = z_o/t_a$ of

$$v_a = \left[\frac{\mu \ln c}{4\pi^2(c^2-1)}\right]^{1/2} \frac{f_c}{\sqrt{f_m}} \frac{(I_o/a)}{\sqrt{\rho}} \qquad (6)$$

The parameters f_c, f_m are current factor and mass swept-up factor /9/. We note the dependence of v_a on $(I_o/a)/\sqrt{\rho}$ which is designated as the drive parameter S. Equations (1) & (2) are integrated step-by-step in time for ς and ι, until $\varsigma = 1$. Then the dynamics move to the radial phase as follows:

S= Current (linear) density over mass density power half

Radial Phase- Four coupled equations (7) to (10)

Inward shock: $$\frac{d\kappa_s}{d\tau} = -\alpha\alpha_1\frac{\iota}{\kappa_p} \tag{7}$$

Elongation: $$\frac{d\zeta_f}{d\tau} = -\frac{2}{\gamma+1}\frac{d\kappa_s}{d\tau} \tag{8}$$

Inward piston:

$$\frac{d\kappa_p}{d\tau} = \frac{\frac{2}{\gamma+1}\frac{\kappa_s}{\kappa_p}\frac{d\kappa_s}{d\tau} - \frac{\kappa_p}{\gamma\iota}\left(1-\frac{\kappa_s^2}{\kappa_p^2}\right)\frac{d\iota}{d\tau} - \frac{1}{\gamma+1}\frac{\kappa_p}{\zeta_f}\left(1-\frac{\kappa_s^2}{\kappa_p^2}\right)\frac{d\zeta_f}{d\tau}}{\frac{\gamma-1}{\gamma} + \frac{1}{\gamma}\frac{\kappa_s^2}{\kappa_p^2}} \tag{9}$$

Current: $$\frac{d\iota}{d\tau} = \frac{1 - \int \iota\, d\tau + \frac{\beta_1}{F} f_c \frac{\zeta_f}{\kappa_p}\frac{d\kappa_p}{d\tau}\iota + \frac{\beta_1}{F} f_c \ln\left(\frac{\kappa_p}{c}\right)\frac{d\zeta_f}{d\tau}\iota - \delta\iota}{1 + f_c\beta - f_c\frac{\beta_1}{F}\zeta_f \ln\left(\frac{\kappa_p}{c}\right)} \tag{10}$$

Radial characteristic speed & Speed Factor

$$\text{where } \beta_1 = \frac{\beta}{\ln c}, F = \frac{z_o}{a} \quad (11)$$

and the ratio of the characteristic axial transit time to characteristic pinch time

$$\alpha_1 = \frac{t_a}{t_p} = \frac{[(\gamma+1)(c^2-1)]^{1/2}}{\sqrt{\ln c}} \frac{F\sqrt{f_{mr}}}{2\sqrt{f_m}} \quad (12)$$

$$\text{Hence } t_p = \frac{4\pi}{[\mu(\gamma+1)]^{1/2}} \frac{\sqrt{f_{mr}}}{f_c} \frac{\sqrt{\rho}}{(I_o/a)} a \quad (13)$$

and characteristic pinch time a/t_p is

$$v_p = \frac{[\mu(\gamma+1)]}{4\pi} f_c \frac{I_o/a}{\sqrt{\rho}} \quad (14)$$

Radial characteristic speed & Speed Factor

$$\text{where } \beta_1 = \frac{\beta}{\ln c}, F = \frac{z_o}{a} \qquad (11)$$

and the ratio of the characteristic axial transit time to characteristic pinch time

$$\alpha_1 = \frac{t_a}{t_p} = \frac{[(\gamma+1)(c^2-1)]^{1/2}}{\sqrt{\ln c}} \frac{F\sqrt{f_m}}{2\sqrt{f_{mr}}} \qquad (12)$$

$$\text{Hence } t_p = \frac{4\pi}{[\mu(\gamma+1)]^{1/2}} \frac{\sqrt{f_{mr}}}{f_c} \frac{\sqrt{\rho}}{(I_0/a)} a \qquad (13)$$

and characteristic pinch time a/t_p is

$$v_p = \frac{[\mu(\gamma+1)]}{4\pi} f_c \frac{I_o/a}{\sqrt{\rho}} \qquad (14)$$

S= Current (linear) density over mass density power half

Speed scaling: ratio of radial/axial speed

$$v_r = a/t_r = \frac{[\mu(\gamma+1)]^{1/2}}{4\pi} \frac{f_c}{\sqrt{f_{mr}}} \frac{(I_o/a)}{\sqrt{\rho}}$$

The ratio of characteristic radial and axial speeds is also essentially a geometrical one, modified by thermodynamics. It is $v_r / v_a = \left[\frac{(c^2-1)(\gamma+1)}{4\ln c}\right]^{1/2}$ with a value typically 2.5.

Note that the radial characteristic speed has the same dependence as the axial transit speed on drive factor $S = (I_o/a)/\sqrt{\rho}$.

Note on Time Match Safeguard:

Integration scheme

Integration

Define initial conditions:

$$\tau = 0, \quad \frac{d\zeta}{d\tau} = 0, \quad \zeta = 0, \quad \iota = 0, \quad \int \iota d\tau = 0, \quad \frac{d\iota}{d\tau} = 1, \quad \frac{d^2\zeta}{d\tau^2} = \alpha\sqrt{2/3}$$

Set time increment: D = 0.001

Increment time: $\tau = \tau + D$

Next step values are computed using the following linear approximations:

$$\frac{d\zeta}{d\tau} = \frac{d\zeta}{d\tau} + \frac{d^2\zeta}{d\tau^2} D$$

$$\zeta = \zeta + \frac{d\zeta}{d\tau} D$$

$$\iota = \iota + \frac{d\iota}{d\tau} D$$

$$\int \iota d\tau = \int \iota d\tau + \iota D$$

The 5-phases of the Model code

- axial (phase 1) – 2 coupled equations
- radial inward shock (phase 2) – 4 coupled eqns
- radial RS (phase 3)- 3 coupled equns namely: RS moving outwards, piston moving inwards & circuit
- slow compression radiation phase (phase 4) :

Radiation & heat coupled eqn of motion coupled to circuit eqn; Bennett for temperature & Spitzer for heat; Plasma self-absorption included (P. Lee & Khatak)

- Anomalous resistive phase (Phase 4a) – 3 fitting regimes
- the expanded axial post-pinch phase (phase 5)

Crucial technique of the code: Current Fitting:

The computed current is fitted to the measured; modifying the computation at each step of the fitting;
thus connecting the physics-based model with the reality of the experiment

Philosophy of Current fitting 1/3

- The current trace of the focus is the best indicators of gross performance.
- The exact time profile of the current trace is governed by the bank parameters, the focus tube geometry and the operational parameters.
- It depends on the mass swept-up and drive current fractions and their variations.
- These parameters determine the dynamics, specifically the axial and radial speeds which in turn affect the profile and magnitudes of the current.
- There are many underlying mechanisms (see following slide) which are not simply modeled. The detailed current profile is influenced by these effects and during the pinch phase also reflects the Joule heating and radiative yields.
- At the end of the pinch phase the profile reflects the sudden transition from a constricted pinch to a large column flow.
- Thus the current powers all dynamic, electrodynamic, thermodynamic and radiation processes in the various phases.
- Conversely all dynamic, electrodynamic, thermodynamic and radiation processes in the various phases affect the current.
- **The current waveform contains information on all the dynamic, electrodynamic, thermodynamic and radiation processes that occur in the various phases.**
- This explains the importance attached to matching the computed total current trace to the measured total current trace in the procedure adopted by the Lee model code.
- **Once matched, the fitted model parameters assure that computation proceeds with all physical mechanisms accounted for, in the gross energy & mass balance sense.**

Philosophy of Current fitting 3/3

All inaccurate model effects are accounted for by the fitting:

Known effects that might deviate from our modelling include:

1. Geometrical, including our assumed geometry
2. Our assumed structures and distributions
3. Mass shedding & current sheet CS porosity
4. Current shedding, fragmenting, leakage & inclination
5. Non uniformity & inhomogeneity of CS and plasma; boundary layer effects
6. Radiation & thermodynamics
7. Ejection of mass caused by necking curvatures

Once current-fitted, also unspecified and unknown effect are also accounted for in terms of energy and mass.

Philosophy of Current fitting 2/3

- So we relate to reality through a measured current trace
- computed current waveform is adjusted to fit measured current waveform
- Adjustment by model parameters f_m, f_c, f_{mr}, f_{cr}; account for **all factors** affecting mass flow and force field flows not specifically modelled including all KNOWN and UNKNOWN effects.
- When adjustments are completed so that the computed waveform fit the measured waveform, the **computed system is energetically** and **mass-wise equivalent to the real system.**

Insights

- Limitation to Pinch Current and Yields- **S Lee & S H Saw: Appl Phys Letts. 92 (2008)** **Note also: M Trunk Plasma Physics, 17, 237 (1975)**
- Neutron Yield Scaling-sub kJ to 1 MJ-**J Fusion Energy 27 (2008) S Lee & S H Saw-** multi-MJ- **PPCF 50 (2008) S Lee**
- Neon Soft x-ray Scaling- **PPCF 51 (2009) S Lee, S H Saw, P Lee, R S Rawat**
- Neutron Yield Saturation- **Appl Phys Letts. 95 (2009) S Lee**

Simple explanation of major obstruction to progress

Benchmarking Fast Ion Beams and scaling laws-S Lee, S H Saw

From Measured Current Waveform to Modelling for Diagnostics

Procedure to operate the code:

Step 1: Configure the specific plasma focus,

Input:

- **Bank parameters, L_0, C_0 and stray circuit resistance r_0;**
- **Tube parameters b, a and z_0 and**
- **Operational parameters V_0 and P_0 and the fill gas**

Step 2: Fitting the computed current waveform to the measured waveform-(connecting with reality)

- A measured discharge current I_{total} waveform for the specific plasma focus is required
- The code is run successively. At each run the computed I_{total} waveform is fitted to the measured I_{total} waveform by varying model parameters f_m, f_c, f_{mr} and f_{cr} one by one, one step for each run, until computed waveform agrees with measured waveform.
- 1. Fitting static inductance Lo and stray resistance ro.

  This is done by matching current risetimes and current amplitudes
- 2. The 5-Point Fit:
- First, the axial model factors f_m, f_c are adjusted (fitted) until
  - (1) computed rising slope of the I_{total} trace and
  - (2) the rounding off of the peak current as well as
  - (3) the peak current itself

  are in reasonable (typically very good) fit with the measured I_{total} trace.
- Next, adjust (fit) the radial phase model factors f_{mr} and f_{cr} until
  - (4) the computed slope and
  - (5) the depth of the dip

  agree with the measured I_{total} waveform.

Example of current fitting: Given any plasma focus : e.g. PF1000

- Bank parameters: L_0=20nH (nominal) ; C_0=1332 μF; r_0=not given (try 1 mΩ)
- Tube parameters: b=16 cm, a=11.55 cm, z_0=60cm
- Operation parameters: V_0=27kV, P_0=3.5 Torr in D

The UPFLF (Lee code) is configured (by keying figures into the **configuration panel** on the EXCEL sheet) as the PF1000

Step I.2. Configure the code as the PF1000 using given parameters; note those parameters (in red) that are not certain or guessed

Start Configuration						
Given:	L_0 nH	C_0 uF	b cm	a cm	z_0 cm	r_0 mΩ
	20	1332	16	11.55	60	**1**
	fm	fc	fmr	fcr		
	0.1	**0.7**	**0.2**	**0.7**		
	V_0 kV	P_0 Torr	MW	A	Atom-molecule	
	27	3.5	4	1	2	

Fitting PF1000

1000 kJ machine

Big Plasma Focus

Fire the PF1000, compare computed current waveform with measured current waveform

1. Use typical trial values of f_m, f_c, f_{mr}, f_{cr}; use given value of L_0 and guess value of r_0;
Result: **computed current risetime too short; need to increase L_0-** risetime~$L_0^{0.5}$

Lo	Co	b	a	zo	ro mOhm
20	1332	16	11.55	60	1
massf	currf	massfr	currfr	Model Parameters	
0.07	0.7	0.16	0.7		
Vo	Po	MW	A	At-1 mol-	Operational
27	3.5	4	1	2	Parameters

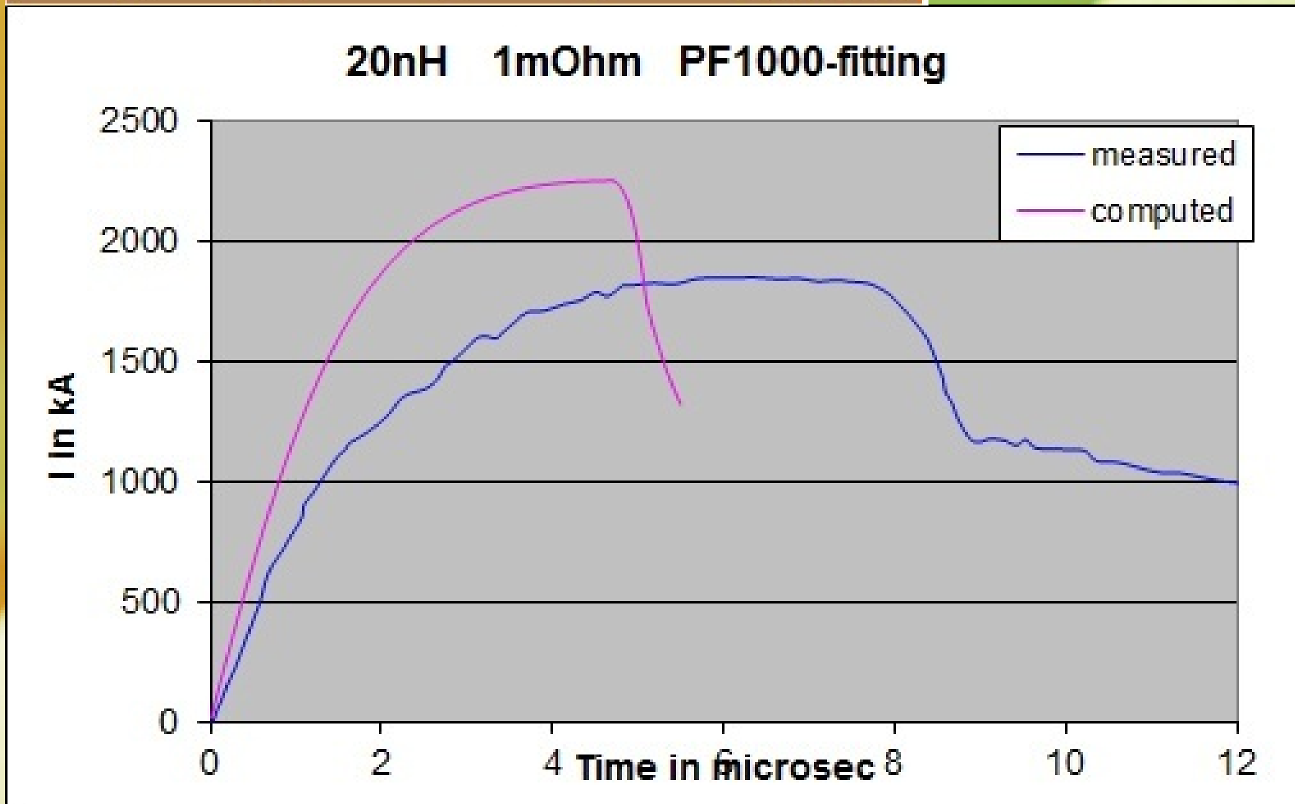

2. **Increase L_0 to 25 nH**, computed **risetime increases**, fits better; but not enough. Need to increase L_0 further

Lo	Co	b	a	zo	ro mOhm
25	1332	16	11.55	60	1
massf	currf	massfr	currfr	Model Parameters	
0.07	0.7	0.16	0.7		
Vo	Po	MW	A	At-1 mol-	Operational
27	3.5	4	1	2	Parameters

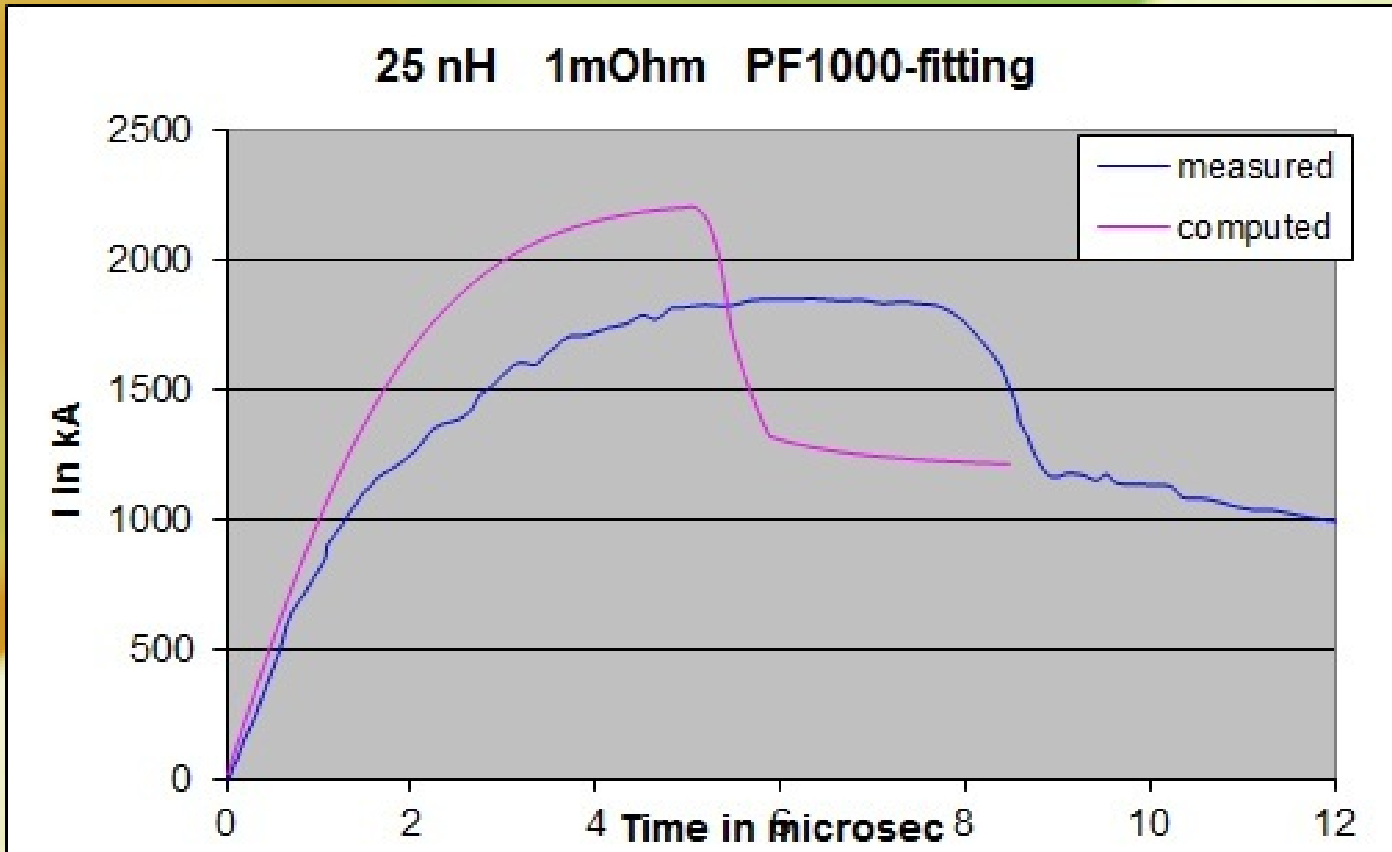

3. Increase L_0 to 30 nH, fits better. Next note computed current too high; that suggests to increase r_0

Lo	Co	b	a	zo	ro mOhm
30	1332	16	11.55	60	1
massf	currf	massfr	currfr	Model Parameters	
0.07	0.7	0.16	0.7		
Vo	Po	MW	A	At-1 mol-	Operational
27	3.5	4	1	2	Parameters

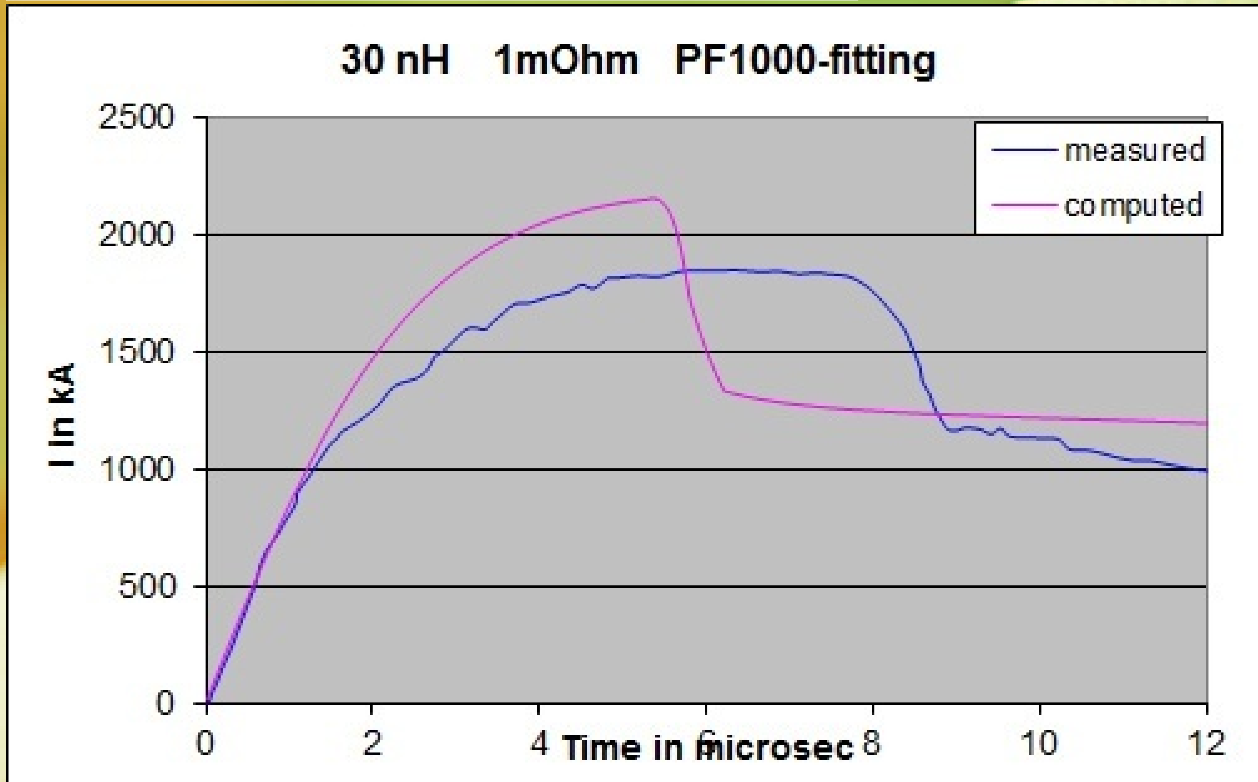

4. Increase r_0 to 3 mΩ, that drops the current and the fit is better. Try increase r_0 further

Lo	Co	b	a	zo	ro mOhm
30	1332	16	11.55	60	3
massf	currf	massfr	currfr	Model Parameters	
0.07	0.7	0.16	0.7		
Vo	Po	MW	A	At-1 mol-	Operational
27	3.5	4	1	2	Parameters

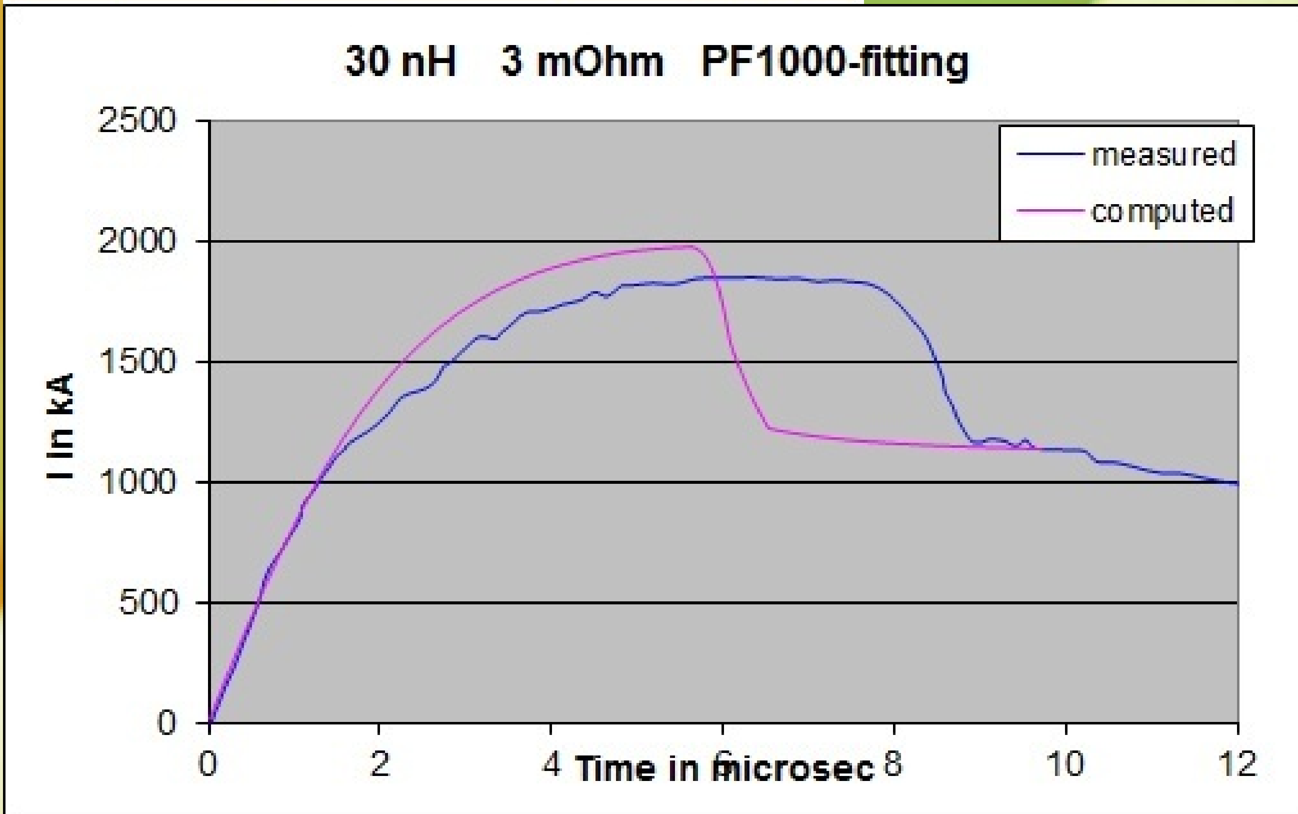

5. Increase r_0 to 5 mΩ; fit of current rise slope is now quite good. For the moment fit of L_0 and r_0 looks OK; although may need to come back later.
Next note radial phase comes far too early; that means axial speed too fast.
To reduce axial speed, increase axial mass factor f_m

Lo	Co	b	a	zo	ro mOhm
30	1332	16	11.55	60	5
massf	currf	massfr	currfr	Model Parameters	
0.07	0.7	0.16	0.7		
Vo	Po	MW	A	At-1 mol-	Operational
27	3.5	4	1	2	Parameters

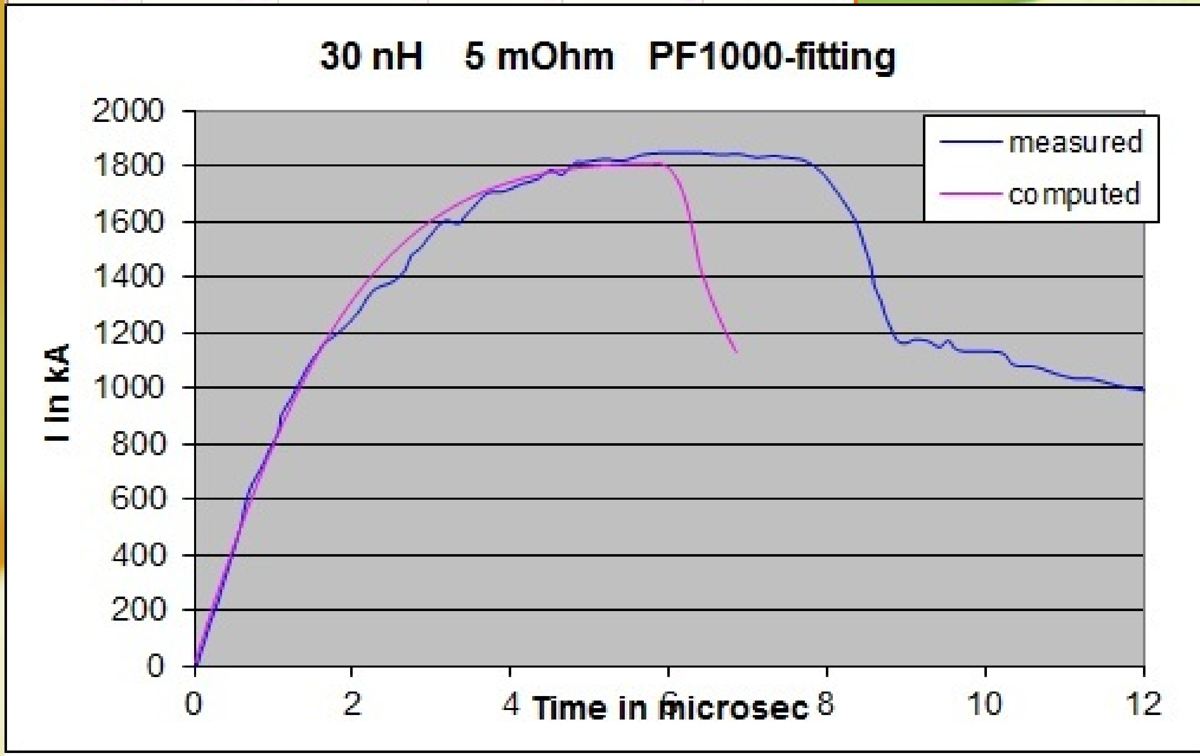

INTI INTERNATIONAL UNIVERSITY
LAUREATE INTERNATIONAL UNIVERSITIES
School and Training Course on Dense Magnetized Plasma as a Source of Ionizing Radiations, their Diagnostics and Applications
8-12 October 2012, ICTP, Trieste
IPFS Institute For Plasma Focus Studies
• Knowledge Should Be Freely Accessible To All •

6. Increase axial f_m to 0.1; note improvement to fit; but axial speed still too fast. Need to increase f_m further. Note, also that reducing the speed increases the current

Lo	Co	b	a	zo	ro mOhm
30	1332	16	11.55	60	5
massf	currf	massfr	currfr	Model Parameters	
0.1	0.7	0.16	0.7		
Vo	Po	MW	A	At-1 mol-	Operational
27	3.5	4	1	2	Parameters

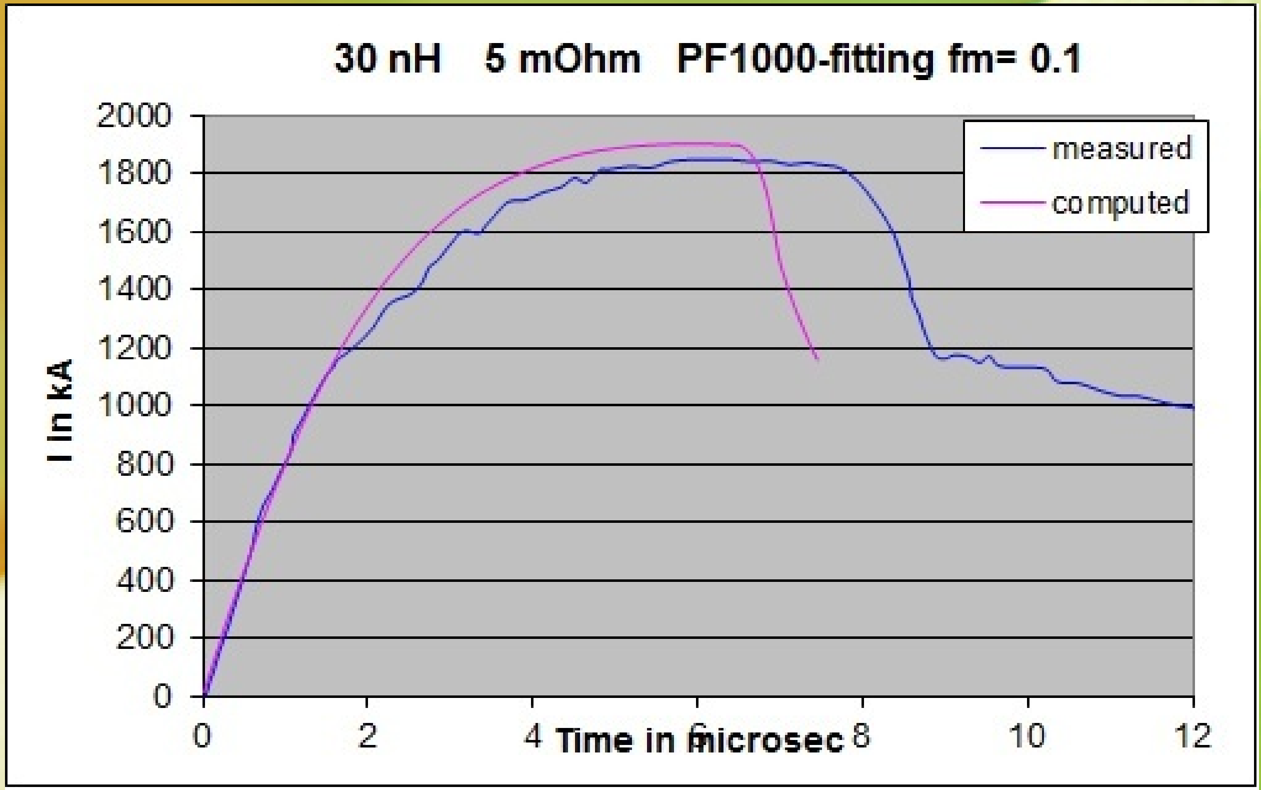

7. Increase f_m to 0.13, note that computed radial phase starts later and fit is better; but still not enough. Also note that current has gone higher- due to the reduced loading because of lower speed. Note: lower speed leads to higher current. Suggest increase f_m, which will slow axial speed and increase current further; so at same time need to increase r_0

Lo	Co	b	a	zo	ro mOhm
30	1332	16	11.55	60	5
massf	currf	massfr	currfr	Model Parameters	
0.13	0.7	0.16	0.7		
Vo	Po	MW	A	At-1 mol-	Operational
27	3.5	4	1	2	Parameters

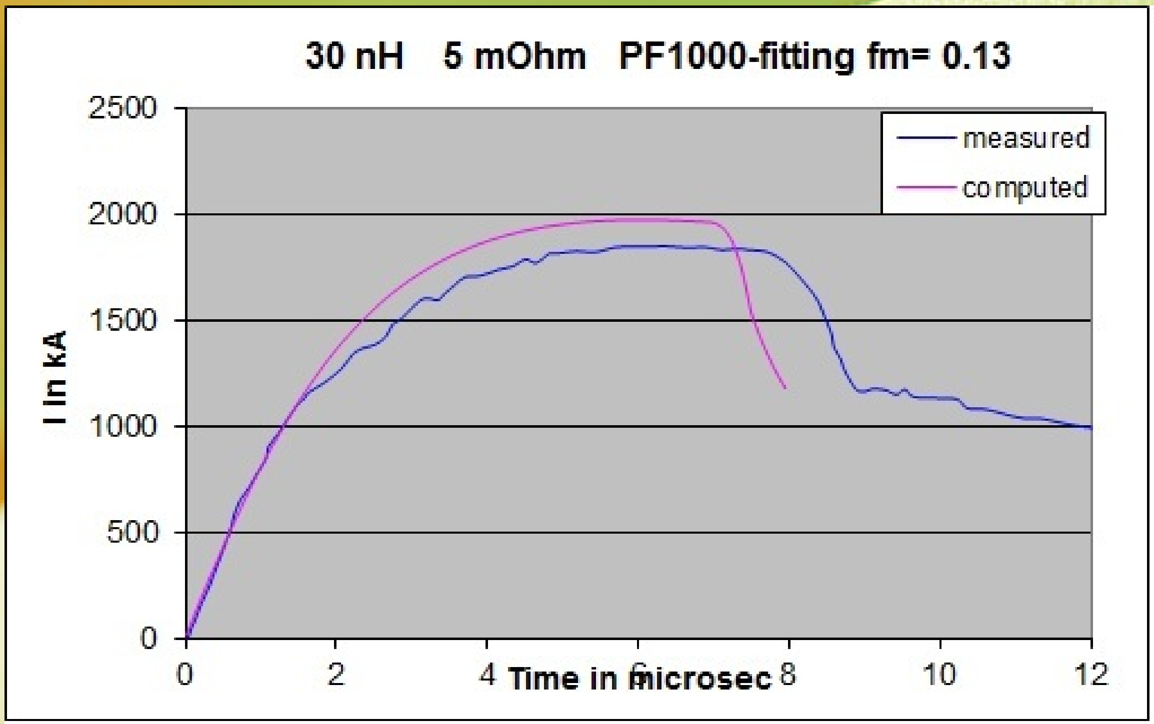

8. Increase f_m to 0.14 at same time increase r_0 to 6 mΩ; fit is now better but current still too high; the computed radial start point is still slightly early; but if we increase r_0 the current will drop and the speed will reduce. So suggest increase r_0 slightly.

Lo	Co	b	a	zo	ro mOhm
30	1332	16	11.55	60	6
massf	currf	massfr	currfr	Model Parameters	
0.14	0.7	0.16	0.7		
Vo	Po	MW	A	At-1 mol-2	Operational
27	3.5	4	1	2	Parameters

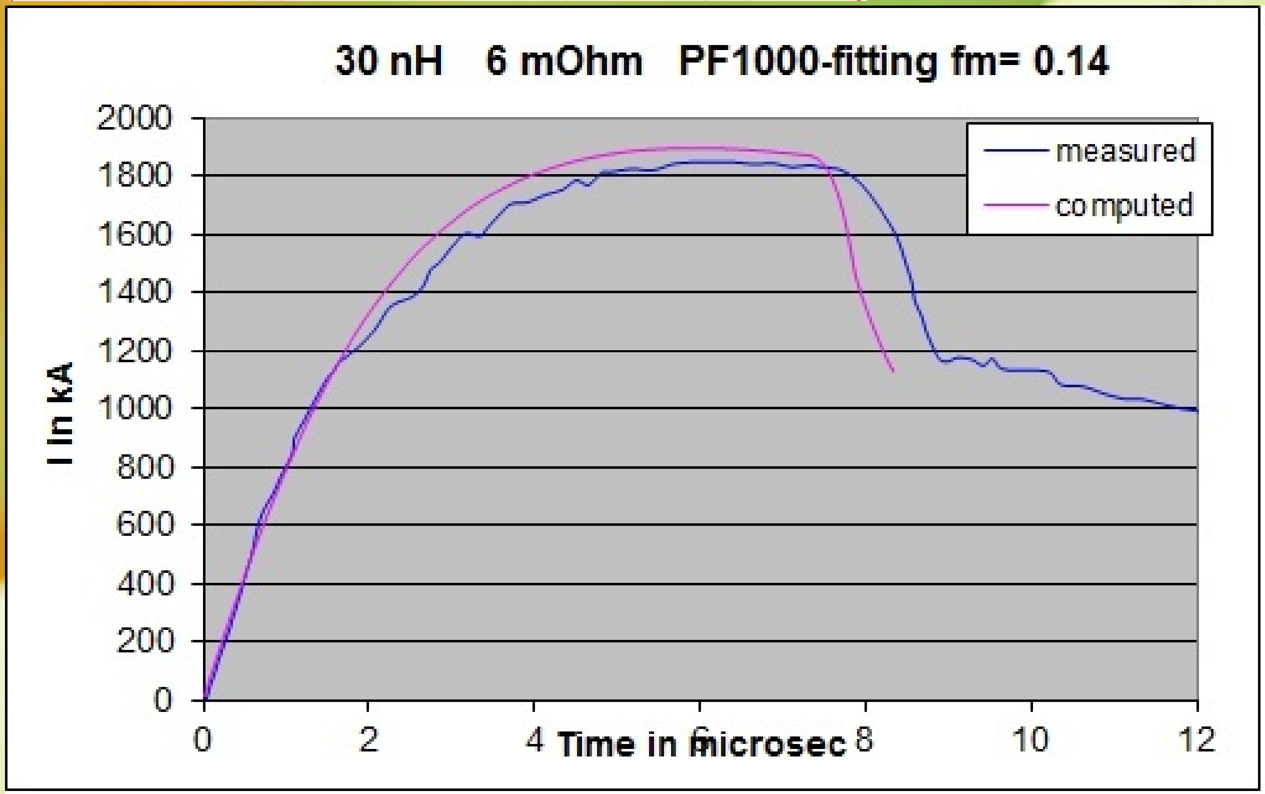

9. Increase r_0 to 6.3 mΩ. Note that the computed current has dropped enough for the rising slope (particularly the top part of the rising slope) and the flattened top to agree very well. Also the computed current dip start (roll off) agrees very well with the measured current dip start. Thus L_0 and r_0 fitted; also f_m is fitted.

Lo	Co	b	a	zo	ro mOhm
33	1332	16	11.55	60	6.3
massf	currf	massfr	currfr	Model Parameters	
0.14	0.7	0.16	0.7		
Vo	Po	MW	A	At-1 mol-	Operational
27	3.5	4	1	2	Parameters

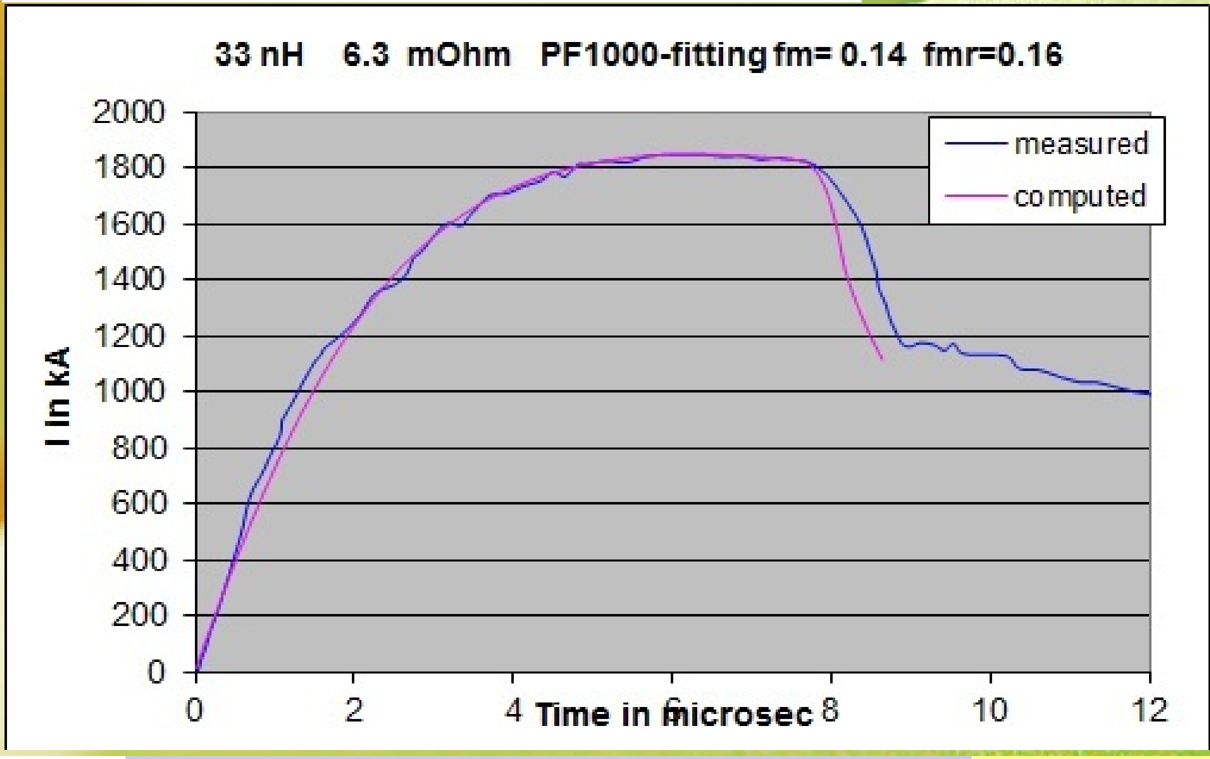

10 Next, to fit the radial phase. Note last slide computed slope of dip is much too steep than measured dip slope. This means that the computed speed is too high. To reduce the radial speed, increase f_{mr}; try 0.25. Note improvement; the computed slope is now less steep and agrees better with the measured; need to increase f_{mr} further.

Lo	Co	b	a	zo	ro mOhm
33	1332	16	11.55	60	6.3
massf	currf	massfr	currfr	Model Parameters	
0.14	0.7	0.25	0.7		
Vo	Po	MW	A	At-1 mol-	Operational
27	3.5	4	1	2	Parameters

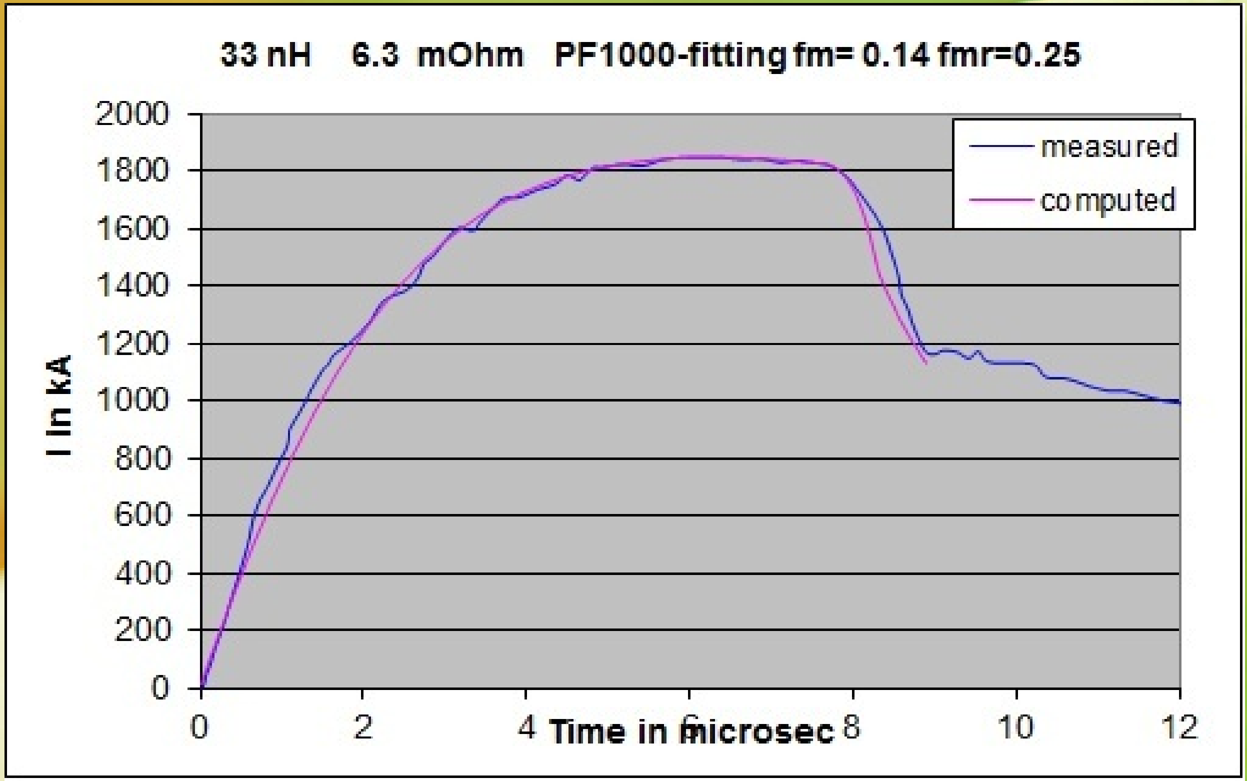

11. Increase f_{mr} to 0.34; Note that the average slope of the computed current dip is now very close to the average slope of the measured current dip. Note 5 points of agreement: 1. Rising slope; 2. Topping profil;e 3. Top and Ipeak; 4.start of current dip; 5.slope of dip; and 6. Bottom of dip. The fit is good overall.

Lo	Co	b	a	zo	ro mOhm
33	1332	16	11.55	60	6.3
massf	currf	massfr	currfr	Model Parameters	
0.14	0.7	0.34	0.7		
Vo	Po	MW	A	At-1 mol-	Operational
27	3.5	4	1	2	Parameters

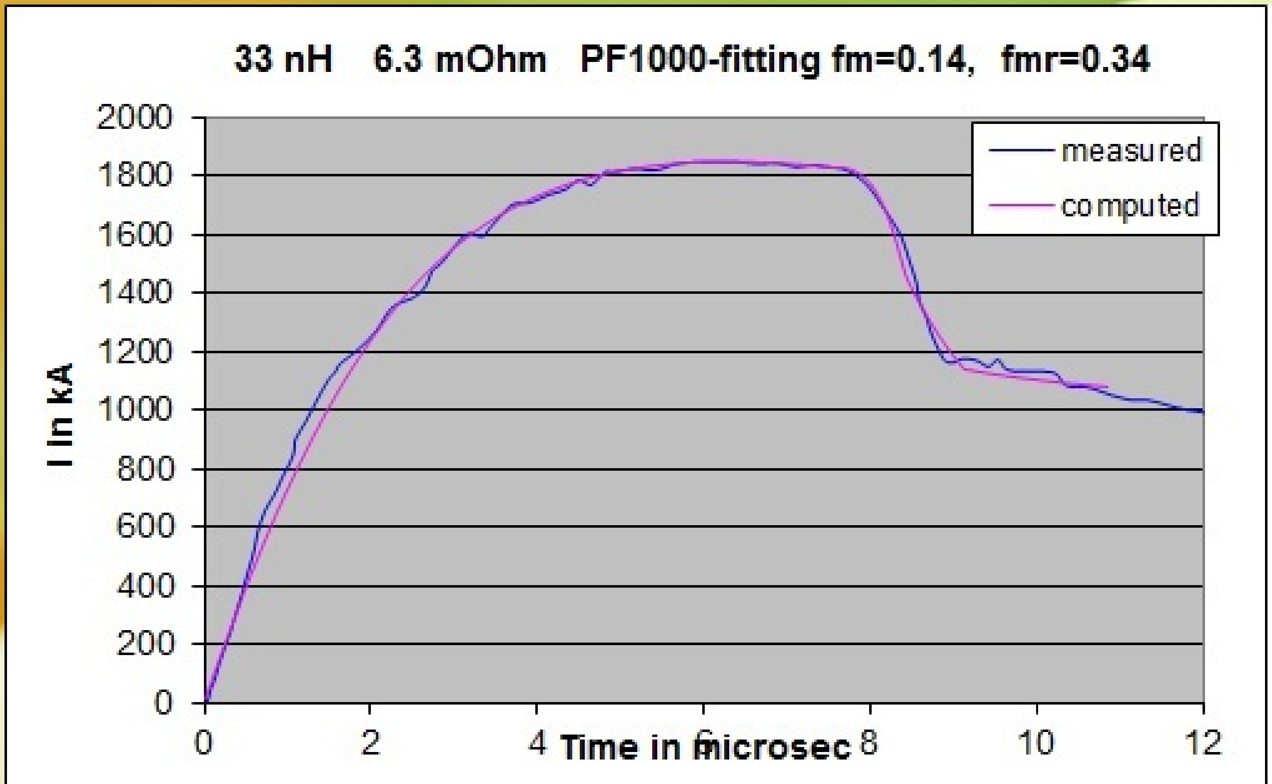

Fitting PF1000 27kV-adjusting model parameters until computed current waveform matches measured (after getting L_0 correct)

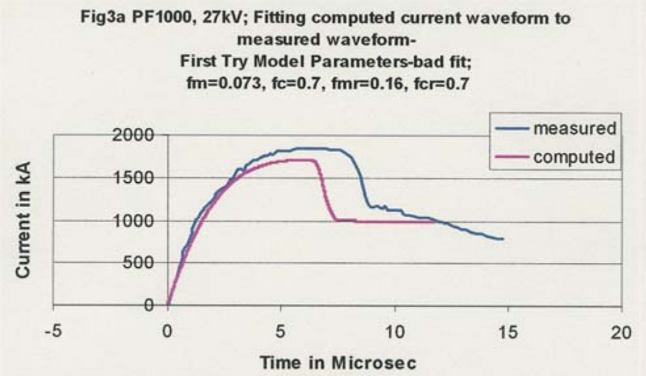

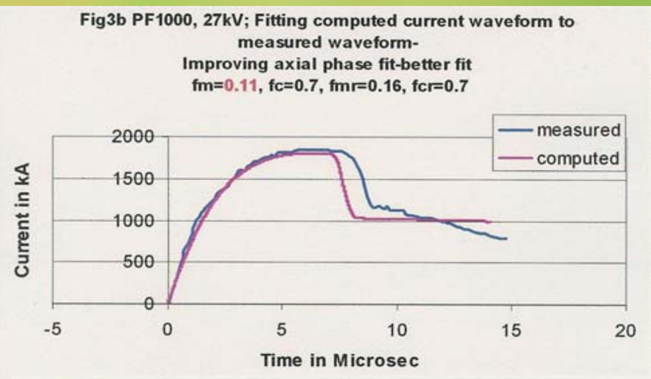

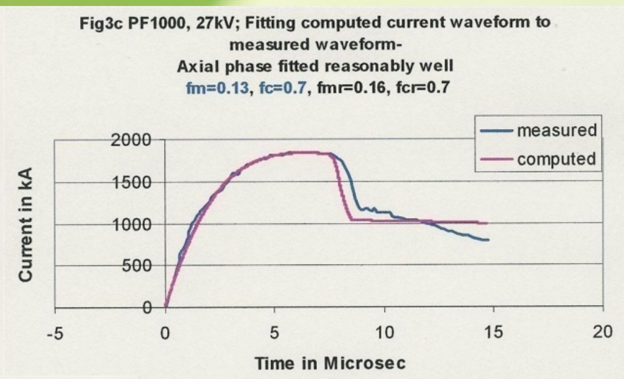

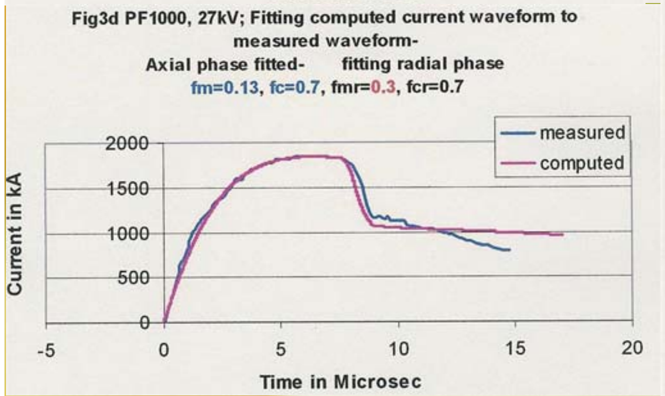

PF1000	Lo nH	Co uF	ro mOhm	b cm	a cm	zo cm	Vo kV	Po torr D2
	33.5	1332	6.3	16	11.55	60	27	3.5

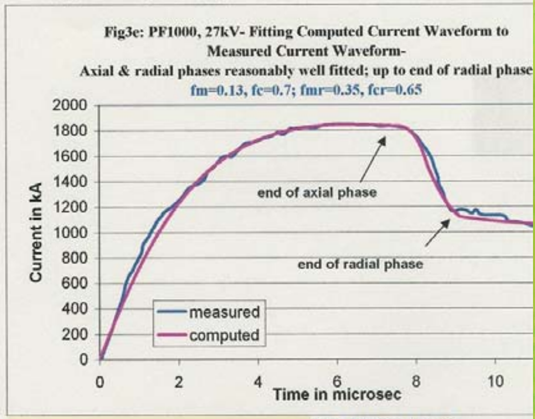

There is good agreement up 9.12 us, the end of the radial phases

Computed neutron yield agrees with those reported in the paper by Gribkov et al.

CLICK ON SI
to see fitted fo

PF1000 fitted results

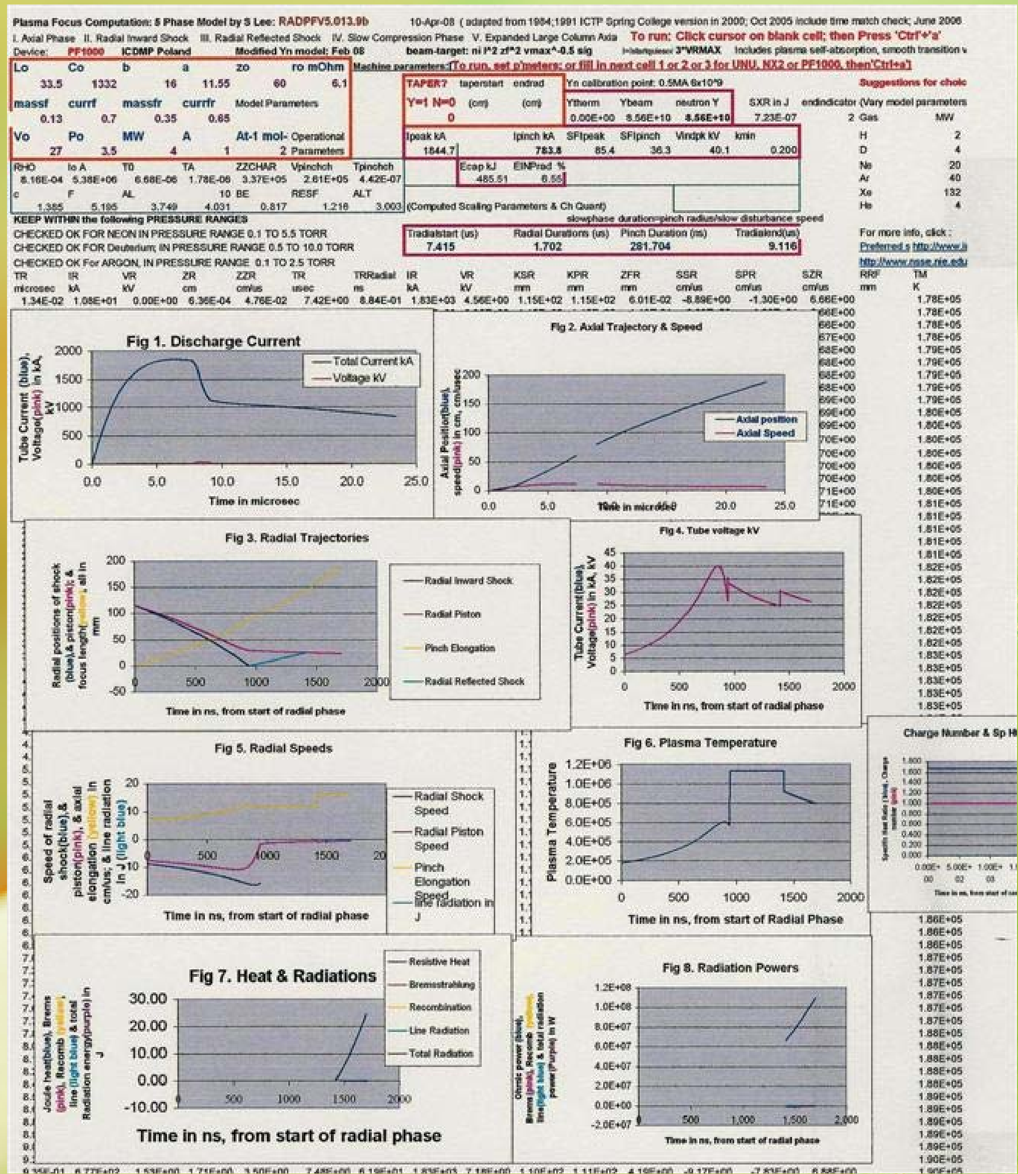

Summary: the 5-point fit 1/2

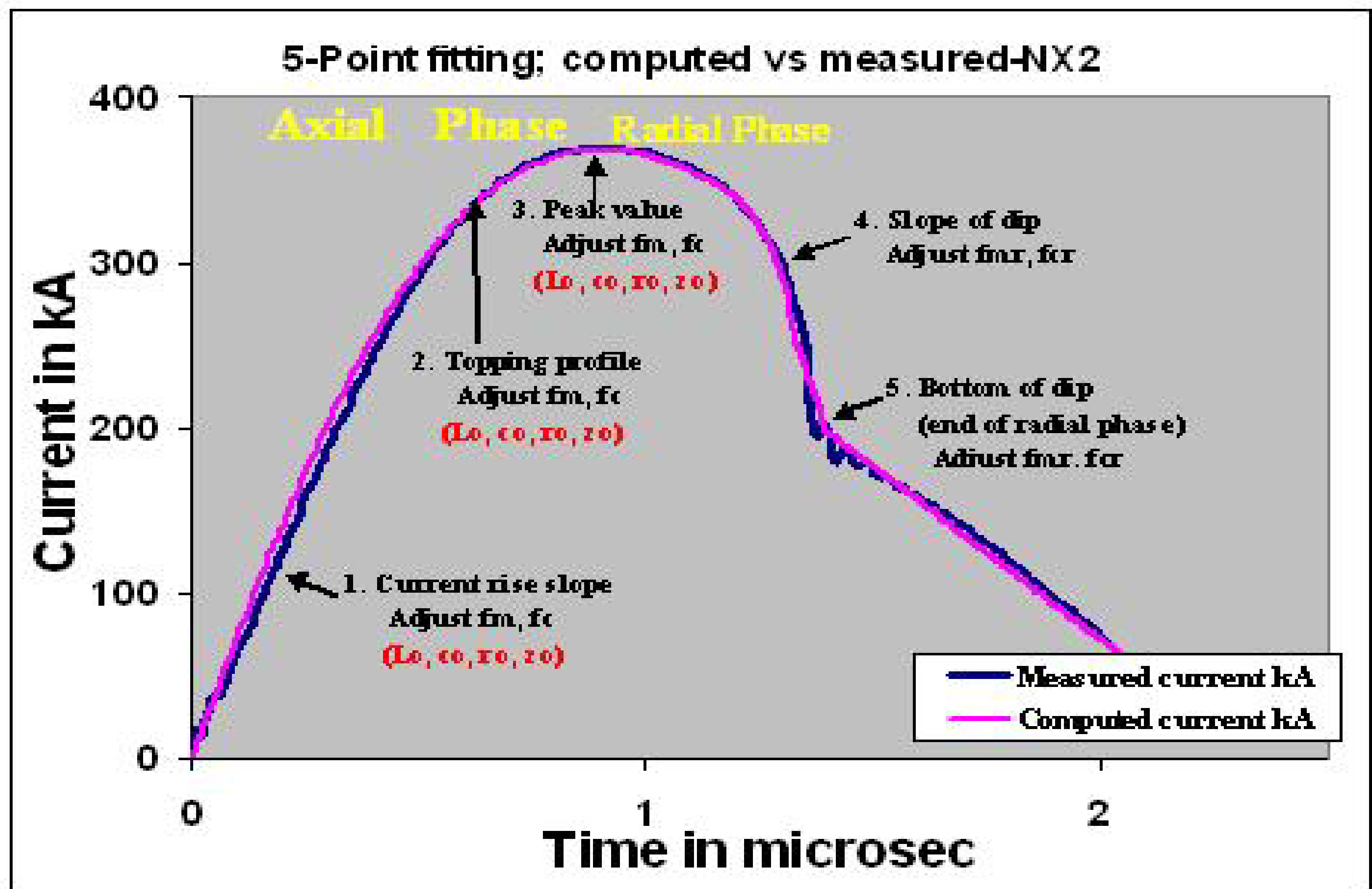

Once fitted: model is energy-wise & mass-wise equivalent to the physical situation 2/2

- All dynamics, electrodynamics, radiation, plasma properties and neutron yields are realistically simulated; so that the code output of these quantities may be used as reference points for diagnostics

Scaling Properties

3 kJ machine

Small Plasma Focus

1000 kJ machine

Big Plasma Focus

Comparing large and small PF's- Dimensions and lifetimes- putting shadowgraphs side-by-side, almost same scale

Comparing UNU ICTP PFF (170 kA) and PF1000 (at 2 MA)- Deuterium 3 Torr

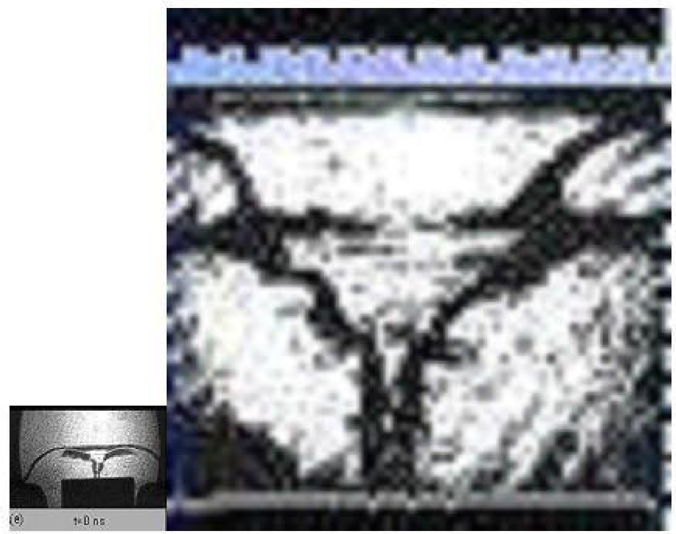

Anode radius	1 cm	11.6 cm
Pinch Radius:	1mm	12mm
Pinch length:	8mm	90mm

Lifetime ~10ns order of ~100 ns

Focus Pinch T, dimensions & lifetime with anode radius ‘a’

Scaling properties-mainly radial phase

- Dimensions and lifetime scales as the anode radius ‘a’.
- r_{min}/a (almost constant at 0.14-0.17)
- z_{max}/a (almost constant at 1.5)
- Pinch duration narrow range 8-14 ns/cm of ‘a’

- **T_{pinch} is measure of energy per unit mass.**

  Quite remarkable that this energy density varies so little (factor of 5) over such a large range of device energy (factor of 1000).

Scaling Properties: Pinch Dimensions & Duration: Compare D & Ne

(Lee, Kudowa 1998, Cairo 2003)

Table 3.

		Deuterium	Neon (for SXR)
minimum radius	r_{min}	0.15a	0.05a
max length (hollow anode)	z	1.5a	1.6a
radial shock transit	t_{comp}	$5 \times 10^{-6}a$	$4 \times 10^{-6}a$
pinch lifetime	t_p	$10^{-6}a$	$10^{-6}a$
Speed factor	SF	90	

Rule-of-thumb scaling properties, (subject to minor variations caused primarily by the variation in c=b/a) over whole range of device

• Axial phase energy density (per unit mass)	constant
• Radial phase energy density (per unit mass)	constant
• Pinch radius ratio	constant
• Pinch length ratio	constant
• Pinch duration per unit anode radius	constant

Computation of Neutron yield (1/2)

- Adapted from Beam-target neutron generating mechanism (ref Gribkov et al)
- A beam of fast deuteron ions close to the anode interacts with the hot dense plasma of the focus pinch column produces the fusion neutrons

Given by:

$$Y_{b-t} = C_n\, n_i I_{pinch}^2 z_p^2 (\ln(b/r_p))\sigma / U^{0.5}$$

where
n_i = ion density
b = cathode radius,
r_p = radius of the plasma pinch column with length z_p,
σ = cross-section of the D-D fusion reaction, n- branch,
U= beam energy, and
C_n = calibration constant

More detailed description:

The beam-target yield is written in the form $Y_{b\text{-}t} \sim n_b n_i (r_p^2 z_p)(v_b \boldsymbol{\sigma}) \tau$ where n_b is the number of beam ions per unit plasma volume, n_i is the ion density, r_p is the radius of the plasma pinch with length z_p, σ is the cross section of the D–D fusion reaction, *n* branch,[18] v_b is the beam ion speed, and τ is the beam-target interaction time assumed proportional to the confinement time of the plasma column.

Total beam energy is estimated[17] as proportional to $L_p I_{pinch}^2$ a measure of the pinch inductance energy, L_p being the focus pinch inductance. Thus, the number of beam ions is $N_b \sim L_p I_{pinch}^2 / v_b^2$ and n_b is N_b divided by the focus pinch volume. Note that $L_p \ln b / r_p z_p$, that[4] $r_p z_p$, and that $v_b U_{1/2}$ where U is the disruption-caused diode voltage.[17] Here, b is the cathode radius.We also assume reasonably that U is proportional to V_{max}, the maximum voltage induced by the current sheet collapsing radially toward the axis.

Computation of Neutron yield (2/2)

Note:

- The D-D cross-section is sensitive to the beam energy in the range 15-150 kV; so it is necessary to use the appropriate range of beam energy to compute σ.
- The code computes induced voltages (due to current motion inductive effects) V_{max} of the order of only 15-50 kV. However it is known, from experiments that the ion energy responsible for the beam-target neutrons is in the range 50-150keV, and for smaller lower-voltage machines the relevant energy could be lower at 30-60keV.
- In line with experimental observations the D-D cross section σ is reasonably obtained by using $\mathbf{U = 3V_{max}}$.
- The model uses a value of C_n =2.7x10^7 obtained by calibrating the yield at an experimental point of 0.5 MA.

Computation of Neon SXR yield (1/2)

Neon SXR energy generated Y_{SXR} = Neon line radiation Q_L

Q_L calculated from:

$$\frac{dQ_L}{dt} = -4.6x10^{-31} n_i^{\,2} Z Z_n^4 \left(\pi r_p^2\right) z_f / T$$

where :

Z_n = atomic number,

n_i = number density ,

Z = effective charge number,

r_p = pinch radius,

z_f = pinch length and

T = temperature

Q_L is obtained by integrating over the pinch duration.

Computation of Neon SXR yield (2/2)

Note:

- The SXR yield is the reduced quantity of generated energy after plasma self-absorption which depends primarily on density and temperature
- The model computes the volumetric plasma self-absorption factor A derived from the photonic excitation number M which is a function of the Z_n, n_i, Z and T.
- In our range of operation the numerical experiments show that the self absorption is not significant.
- Liu Mahe (1999) first pointed out that a temperature around 300 eV is optimum for SXR production. Shan Bing's (2000) subsequent work and our experience through numerical experiments suggest that around 2×10^6 K (below 200 eV) or even a little lower could be better.
- Hence for SXR scaling there is an optimum small range of temperatures

(*T* window). [200-500 eV]

Scaling laws for neutrons from numerical experiments over a range of energies from 10kJ to 25 MJ (1/4)

- To study the neutrons emitted by PF1000-like bank energies from 10kJ to 25 MJ.
- 1) Apply the Lee model code to fit a measured current trace of the PF1000:

  C_0 = 1332 μF, V_0 = 27 kV, P_0 = 3.5 torr D_2; b = 16 cm, a = 11.55 cm or c=1.39; z_0 = 60 cm; external (or static) inductance L_0= 33.5 nH and; damping factor RESF= 1.22 (or stray resistance r_0=6.1 mΩ).

- 2) Apply the Lee code over a range of C_0 ranging from 14 μF (8.5 kJ) to 39960 μF (24 MJ):
  - Voltage, V_0 = 35 kV; P_0 = 10 torr deuterium; RESF = 1.22; ratio c=b/a is 1.39.
  - For each C_0, anode length z_0 is varied to find the optimum z_0.
  - For each z_0, anode radius a_0 is varied to get end axial speed of 10 cm/μs.

Scaling laws for neutrons from numerical experiments over a range of energies from 10kJ to 25 MJ (2/4)

- Fitted model parameters : $f_m = 0.13$, $f_c = 0.7$, $f_{mr} = 0.35$ and $f_{cr}=0.65$.
- Computed current trace agrees very well with measured trace through all the phases: axial and radial, right down to the bottom of the current dip indicating the end of the pinch phase as shown below.

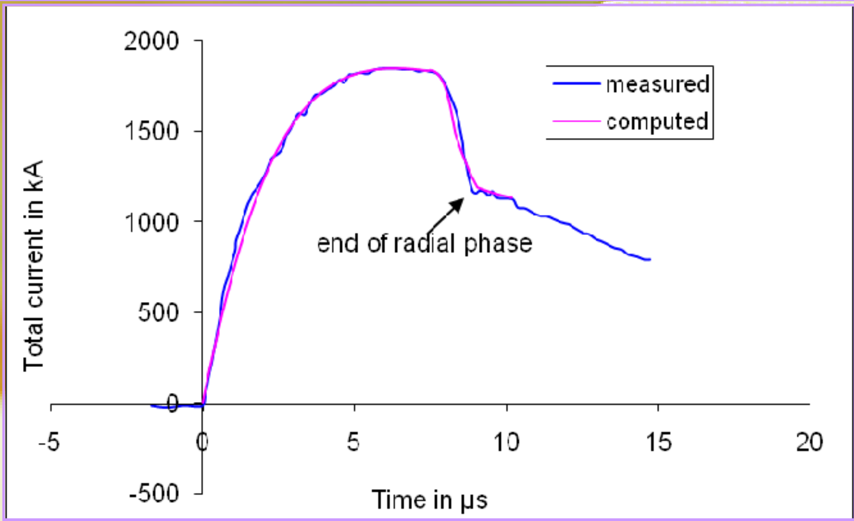

PF1000:
C_0 = 1332 µF; V_0 = 27 kV;
P_0 = 3.5 Torr D_2; b = 16 cm;
a = 11.55 cm; z_0 = 60 cm;
L_0= 33.5 nH; r_0 = 6.1 mΩ or
RESF=1.22.

Scaling laws for neutrons from numerical experiments over a range of energies from 10kJ to 25 MJ (3/4)

- Voltage, V_0 = 35 kV; P_0 = 10 torr deuterium; RESF = 1.22; ratio c=b/a is 1.39.
- Numerical experiments: C_0 ranging from 14 μF(8.5 kJ) to 39960 μF (24 MJ)
- For each C_0, anode length z_0 is varied to find the optimum z_0.
- For each z_0, anode radius a_0 is varied to get end axial speed of 10 cm/μs.

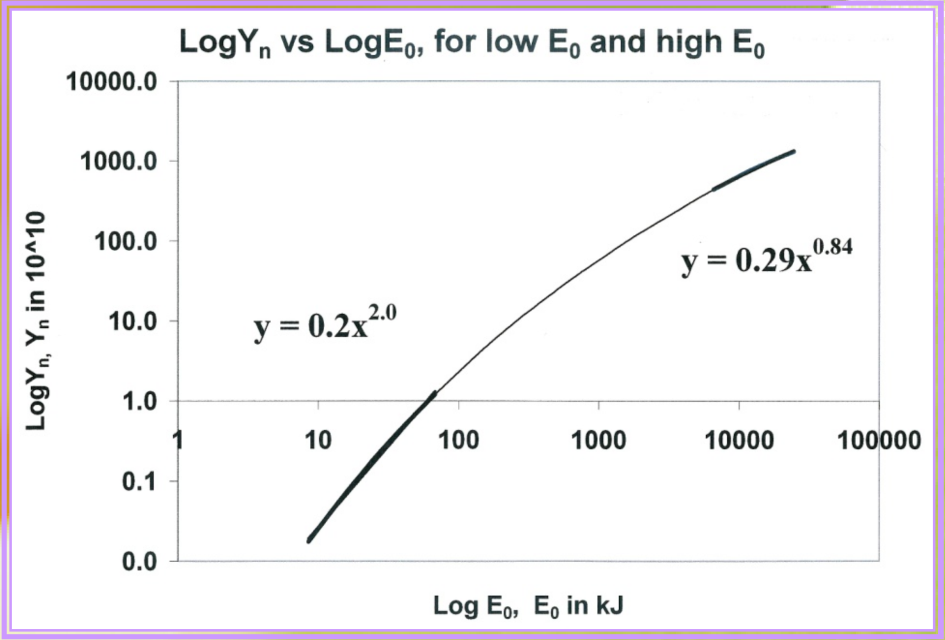

Y_n scaling changes:

- **$Y_n \sim E_0^{2.0}$** at tens of kJ
- **$Y_n \sim E_0^{0.84}$** at the highest energies (up to 25MJ)

Scaling laws for neutrons from numerical experiments over a range of energies from 10kJ to 25 MJ (4/4)

Scaling of Y_n with I_{peak} and I_{pinch}:

- $\mathbf{Y_n = 3.2 \times 10^{11} I_{pinch}^{4.5}}$

  and

- $\mathbf{Y_n = 1.8 \times 10^{10} I_{peak}^{3.8}}$

where $I_{peak} = (0.3\text{-}0.7)$MA

and $I_{pinch} = (0.2 \text{-} 2.4)$MA.

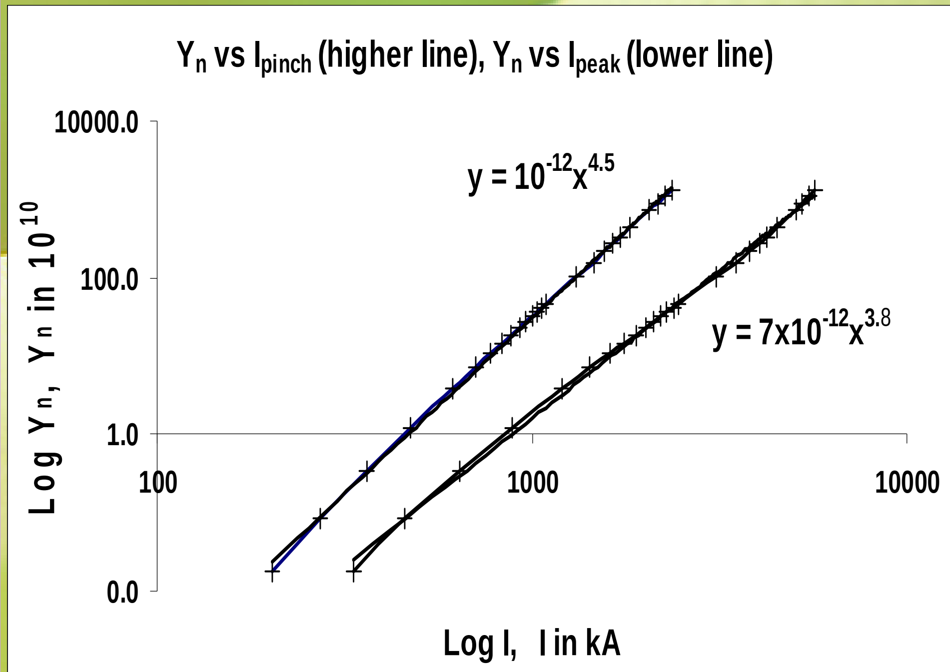

Scaling laws for neon SXR from numerical experiments over a range of energies from 0.2 kJ to 1 MJ (1/4)

- To study the neon SXR emitted by a modern fast bank energies from 0.2 kJ to 1 MJ.
- Apply the Lee model code to a proposed modern fast plasma focus machine:
  1) With optimised values:
     c=b/a =1.5
     V_0= 20 kV
     L_0= 30 nH
     RESF = 0.1
     Model parameters : f_m=0.06, f_c=0.7, f_{mr}=0.16, f_{cr}=0.7.
  2) For C_0 varying from 1 μF (0.2 kJ) to 5000 μF (1MJ):
     For each C_0, vary P_0, z_0, and a_0 to find the optimum Y_{sxr}

Scaling laws for neon SXR from numerical experiments over a range of energies from 0.2 kJ to 1 MJ (2/4)

- Computed Total Current versus Time
- For $L_0 = 30nH$; $V_0 = 20$ kV; $C_0 = 30$ uF; RESF = 0.1; c=1.5
- Model parameters : $f_m = 0.06$, $f_c = 0.7$, $f_{mr} = 0.16$, $f_{cr} = 0.7$
- Optimised a=2.29cm; b=3.43 cm and z_0=5.2 cm.

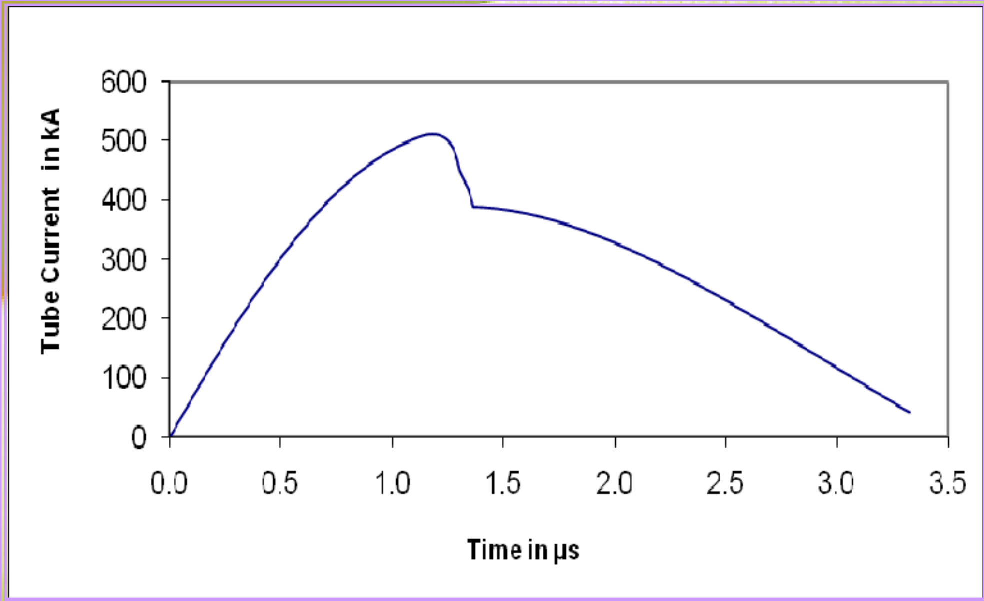

Scaling laws for neon SXR from numerical experiments over a range of energies from 0.2 kJ to 1 MJ (3/4)

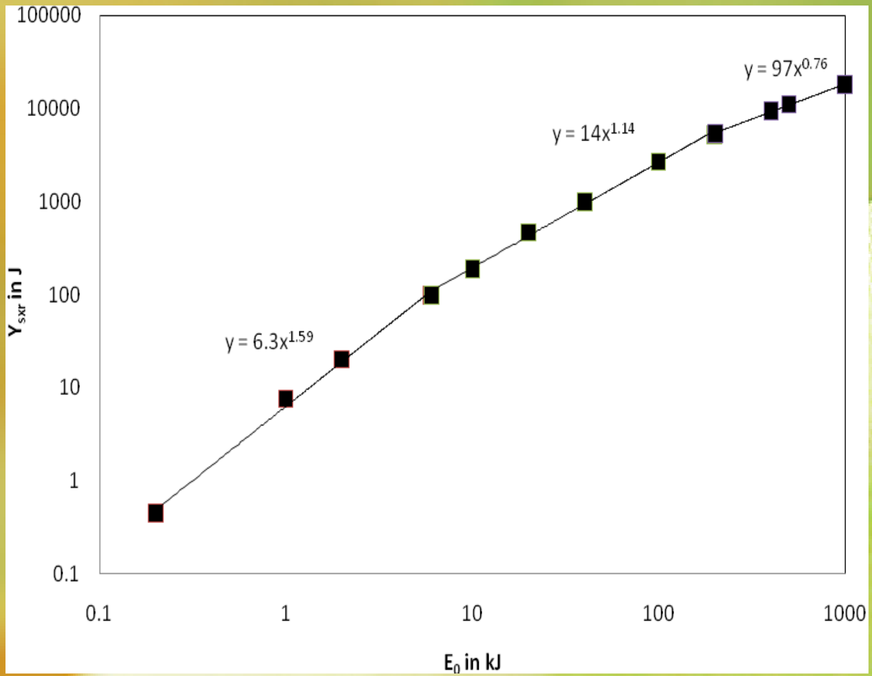

Y_{sxr} scales as:

- $E_0^{1.6}$ at low energies in the sub-kJ to several kJ region.
- $E_0^{0.76}$ at high energies towards 1MJ.

Scaling laws for neon SXR from numerical experiments over a range of energies from 0.2 kJ to 1 MJ (4/4)

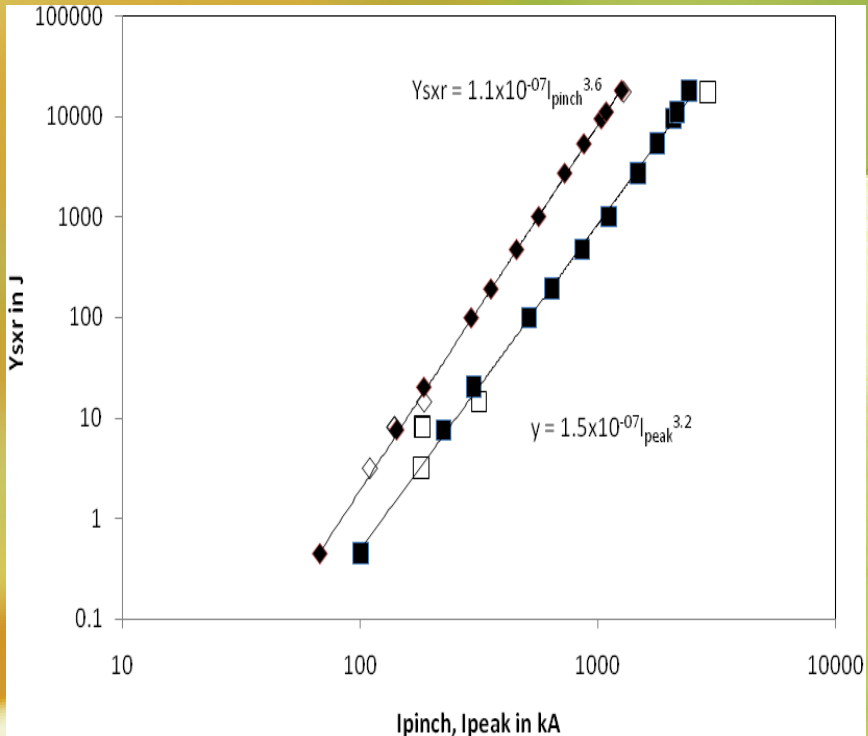

- Scaling with currents
- **$Y_{sxr} \sim I_{peak}^{3.2}$ (0.1–2.4 MA) and**
- **$Y_{sxr} \sim I_{pinch}^{3.6}$ (0.07-1.3 MA)**

- Black data points with fixed parameters RESF=0.1; c=1.5; L_0=30nH; V_0=20 kV and model parameters f_m=0.06, f_c=0.7, f_{mr}=0.16, f_{cr}=0.7.

- White data points are for specific machines with different values for the parameters :c, L_0, V_0 etc.

Summary-Scaling Laws (1/2)

- The scaling laws obtained (at optimized condition) for Neutrons:

- $Y_n \sim E_0^{2.0}$ at tens of kJ to
- $Y_n \sim E_0^{0.84}$ at the highest energies (up to 25MJ)

- $Y_n = 3.2 \times 10^{11} I_{pinch}^{4.5}$ (0.2-2.4 MA)
- $Y_n = 1.8 \times 10^{10} I_{peak}^{3.8}$ (0.3-5.7MA)

Summary-Scaling Laws (2/2)

- The scaling laws obtained (at optimized condition) for neon SXR:

- $\mathbf{Y_{sxr} \sim E_0^{1.6}}$ at low energies
- $\mathbf{Y_{sxr} \sim E_0^{0.8}}$ towards 1 MJ

- $Y_{sxr} \sim I_{\mathbf{peak}}^{3.2}$ (0.1–2.4 MA) and
- $Y_{sxr} \sim I_{pinch}^{3.6}$ (0.07-1.3 MA)

Global scaling law, combining experimental and numerical data- Yn scaling , numerical experiments from 0.4 kJ to 25 MJ (solid line), compared to measurements compiled from publications (squares) from 0.4 kJ to 1 MJ.

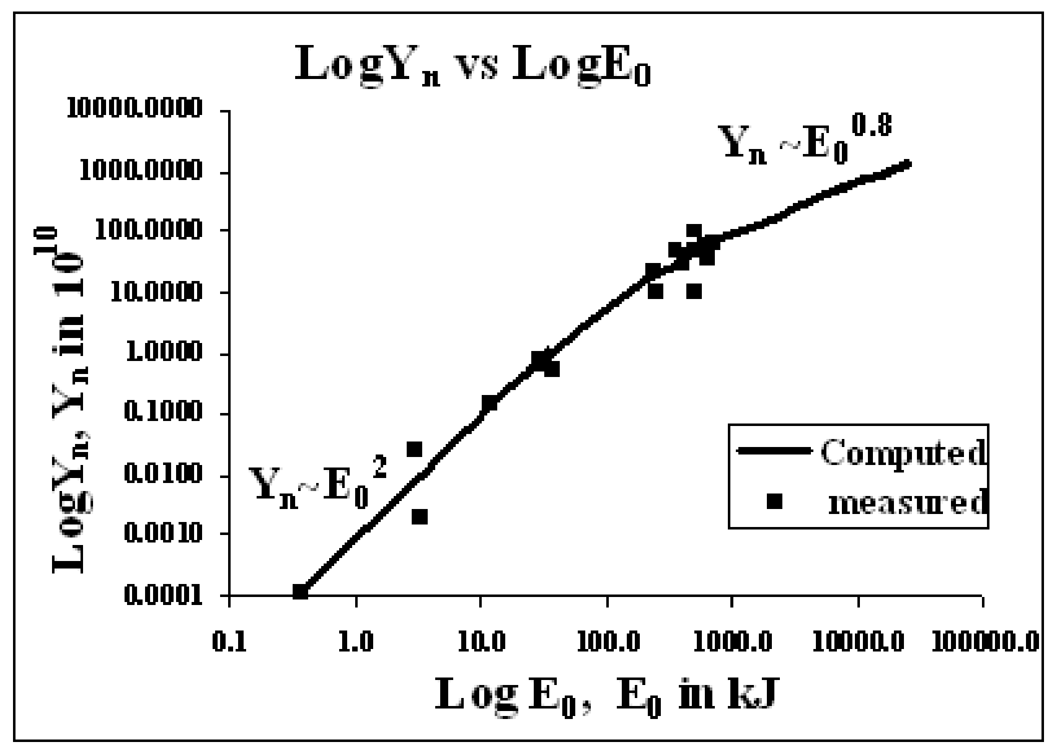

What causes the deterioration of Yield scaling?

What causes current scaling deterioration and eventual saturation? 1/3

- The axial speed loads the discharge circuit with a dynamic resistance
- The same axial speed over the range of devices means the same dynamic resistance constituting a load impedance DR_0
- Small PF's : have larger generator impedance $Z_0=[L_0/C_0]^{0.5}$ than DR_0
- As energy is increased by increasing C_0, generator impedance Z_0 drops

What causes current scaling deterioration and eventual saturation? 2/3

- At E_0 of kJ and tens of kJ the discharge circuit is dominated by Z_0
- Hence as E_0 increases, $I \sim C_0^{-0.5}$
- **At the level typically of 100 kJ, Z_0 has dropped to the level of DR_0; circuit is now no longer dominated by Z_0; and current scaling deviates from $I \sim C_0^{-0.5}$, beginning of current scaling deterioration.**
- At MJ levels and above, the circuit becomes dominated by DR_0, current saturates

Deterioration and eventual saturation of Ipeak as capacitor energy increases

- Axial phase dynamic resistance causes current scaling deterioration as E0 increases

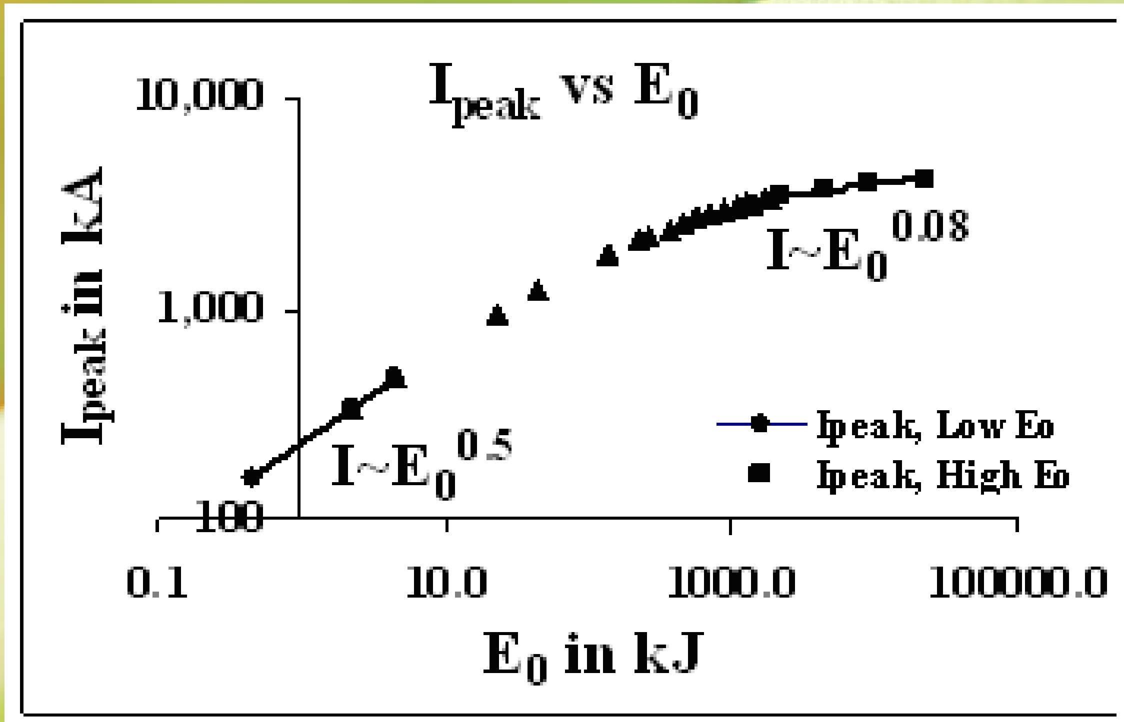

In numerical experiments we showed:

- $Y_n \sim I_{pinch}^{4.5}$
- $Y_n \sim I_{peak}^{3.8}$
- Hence deterioration of scaling of I_{peak} will lead to deterioration of scaling of Y_n.

What causes current scaling deterioration and eventual saturation? 3/3

- Analysis using the Lee model code has thus shown that the constancy of the dynamic resistance causes the current scaling deterioration resulting in the deterioration of the neutron yield and eventual saturation.
- This puts the global scaling law for neutron yield on a firmer footing

Connecting the scaling properties with the global scaling law (1/3)

- At kJ level; experimentally observed$Y_n \sim E_0^2$
- Ideal scaling at the highest convenient voltage V_0: $I \sim V_0 / Z_0$ at low energy level where Z_0 dominates
- leading to $I \sim E_0^{0.5}$ for optimised low L_0
- and $Y_n \sim I_0^4$
- At higher energy around 100kJ, Z_0 domination ends and current deterioration starts

Connecting the scaling properties with the global scaling law (2/3)

- Lower current increase than the ideal leads to lower increase in anode radius 'a'
- This leads to lower increase in pinch volume and pinch duration
- Which leads to lower increase in yield

Connecting the scaling properties with the global scaling law (3/3)

- Finally at very high energies, current hardly increases anymore with further increase in energy
- The anode radius should not be increased anymore; only its length should be increased
- Hence pinch volume and duration also will not increase anymore.

Thus we relate yield scaling deterioration & yield saturation to scaling properties, the fundamental one being the dynamic resistance.

Plasma Focus Numerical Experiments-

Scaling Properties & Scaling Laws

Conclusions

We have used numerical experiments to deduce scaling properties of the plasma focus
We have used numerical experiments to deduce scaling laws for neutrons and neon SXR.
We have connected the scaling laws as a development from the scaling properties.
A Global Scaling Law for neutron yields as a function of storage energies has also been derived from numerical experiments combined with measured data.

A by-product of the numerical experiments are diagnostic reference points.

Papers from Lee model code 1\2

- S Lee and S H Saw, “Pinch current limitation effect in plasma focus,” Appl. Phys. Lett. 92, 2008, 021503.
- S Lee and S H Saw, “Neutron scaling laws from numerical experiments,” J Fusion Energy 27, 2008, pp. 292-295.
- S Lee, P Lee, S H Saw and R S Rawat, “Numerical experiments on plasma focus pinch current limitation,” Plasma Phys. Control. Fusion 50, 2008, 065012 (8pp).
- S Lee, S H Saw, P C K Lee, R S Rawat and H Schmidt, “Computing plasma focus pinch current from total current measurement,” Appl. Phys. Lett. 92 , 2008, 111501.
- S Lee, “Current and neutron scaling for megajoule plasma focus machine,” Plasma Phys. Control. Fusion 50, 2008, 105005, (14pp).
- S Lee and S H Saw, “Response to “Comments on ‘Pinch current limitation effect in plasma focus’”[Appl. Phys. Lett.94,076101 (2009)],” Appl. Phys. Leet.94, 2009, 076102.
- S Lee, S H Saw, L Soto, S V Springham and S P Moo, “Numerical experiments on plasma focus neutron yield versus pressure compared with laboratory experiments,” Plasma Phys. Control. Fusion 51, 2009, 075006 (11 pp).
- S H Saw, P C K Lee, R S Rawat and S Lee, “Optimizing UNU/ICTP PFF Plasma Focus for Neon Soft X-ray Operation,” IEEE Trans Plasma Sci, VOL. 37, NO. 7, JULY (2009)
- Lee S, Rawat R S, Lee P and Saw S H. “Soft x-ray yield from NX2 plasma focus- correlation with plasma pinch parameters” JOURNAL OF APPLIED PHYSICS **106**, 023309 (2009)
- S Lee, S H Saw, P Lee and R S Rawat, “Numerical experiments on plasma focus neon soft x-ray scaling”, Plasma Physics and Controlled Fusion **51**, 105013 (8pp) (2009)

Papers from Lee model code 2\2

- M Akel, S Hawat, S Lee, Numerical Experiments on Soft X-Ray Emission Optimization of Nitrogen Plasma in 3 kJ Plasma Focus Using Modified Lee Model, J Fusion Energy DOI 10.1007/s10894-009-9203-4 First online Tuesday, May 19, 2009
- M Akel, S Hawat, S Lee, Pinch Current and Soft x-ray yield limitation by numerical experiments on Nitrogen Plasma Focus, J Fusion Energy DOI 10.1007/s10894-009-9238 first online 21 August 2009
- S. Lee. Neutron Yield Saturation in Plasma Focus-A fundamental cause.

  Appl Phys Letts (2009) 95, 151503 93..
- M. Akel, Sh. Al-Hawat, S. H. Saw and S. Lee. Numerical Experiments on Oxygen Soft X- Ray Emissions from Low Energy Plasma Focus Using Lee Model J Fusion Energy DOI 10.1007/s10894-009-9262-6 First online 22 November 2009
- Sing Lee and Sor Heoh Saw Numerical Experiments providing new Insights into Plasma Focus Fusion Devices-*Invited Review Paper: for Energy: special edition on "Fusion Energy"*

  Energies 2010, *3*, 711-737; doi:10.3390/en3040711-Published online 12 April 2010
- S H Saw, S Lee, F Roy, PL Chong, V Vengadeswaran, ASM Sidik, YW Leong & A Singh-

  In-situ determination of the static inductance and resistance of a plasma focus capacitor bank –Rev Sci Instruments (2010) 81, 053505
- S H Saw and S Lee, *Scaling the Plasma Focus for Fusion Energy Considerations*- Int. J. Energy Res. (2010) Int. J. Energy Res. (2010) View this article online at wileyonlinelibrary.com. DOI: 10.1002/er.1758
- S H Saw and S Lee- Scaling laws for plasma focus machines from numerical experiments
- Invited paper *Energy and Power Engineering*, 2010, 65-72 doi:10.4236/epe.2010.21010
- Published Online February 2010 (http://www.scirp.org/journal/epe)

Thank You

Numerical experiments with Bora- hands-on

S H Saw

Today 10 October 2012

2pm-4pm (2 hrs)

Summary

- For this exercise we will fit BORA computed current waveform to match a BORA measured current waveform.
- From fitting the rising slope (and the risetime) of the current we obtain the static inductance L_0.
- From the fit of rising profile and the topping profile (including scaling the measured peak to the computed peak) we obtain the bank stray resistance r_0.
- From fitting the axial mass factor f_m and radial mass factor f_{mr} (where necessary also fitting current factors f_c and f_{cr}) we obtain a good overall fit; fixing the dynamics of Bora.
- The final fitting produces from the code realistic results of I_{peak}, I_{pinch}, axial and radial dynamics and pinch properties.

Data for BORA is taken from the following paper:

Dense Plasma Focus "Bora" operational at The Abdus Salam International Centre for Theoretical Physics and experiments provided with the device
V.A. Gribkov, M.V. Chernyshova, A. Cicuttin, M.L. Crespo,
R.A. Miklaszewski, M. Scholz, A.E. Shapiro, K. Tomaszewski, C. Tuniz

Data

1. Capacitance C_0=**24.4 μF** (from pg 15 Table 1)
2. Chamber: cathode radius b=**2.5 cm**; anode radius a=**1.5** cm (pg 65 Fig 62)

   'axial' length z_0=3.5 cm (nominal) curved; will be fitted as an equivalent straight axial length
3. Current derivative trace; (from pg 84 Fig 89) - bottom most trace is used; as this is the trace with effectively the whole trace visible and distinguishable.

This trace is also stated to be of a properly synchronised shot (4 PSS switches properly synchonised) so that each trace is a proper PROFILE representation of the total circuit current.

Current derivative trace: (from pg 84 Fig 89)

The final conditioning of the device has resulted in its proper operation at 17-18 kV with deuterium pressure of about 10 mbar. Corresponding oscilloscope traces obtained by miniature magnetic probes installed near each of our 4 PSSs are presented in Fig. 89.

From this picture one may see that the rise-time of current of our main discharge is equal to about 1.5 μs with the "peculiarity" of the current positioned in a proper place at the moment of 1.8 microsecond from the start of the discharge. By means of Rogowski coil we have measured the amplitude of our discharge current. With 3 capacitors and maximal achievable voltage (19.5 kV) supplied by our charger we obtained the current magnitude equal to 234 kA.

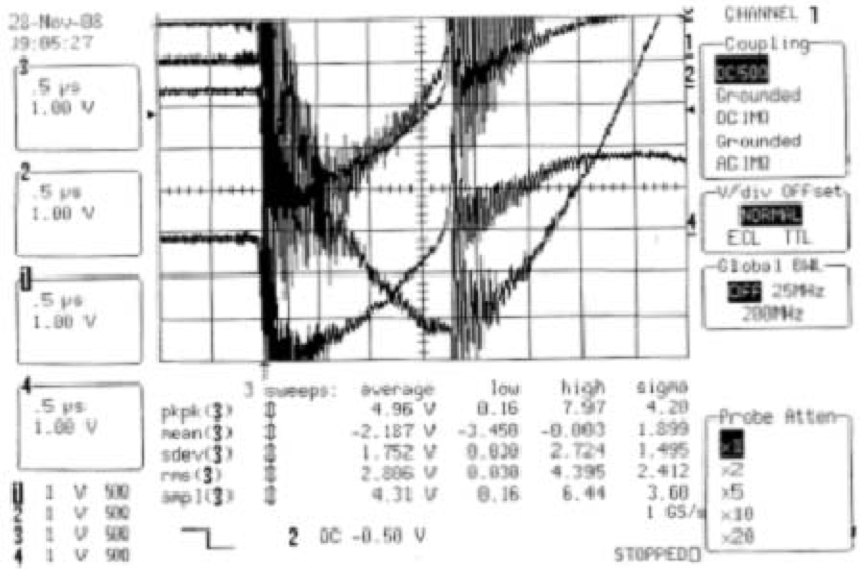

Fig. 89 Oscilloscope traces of the discharge current derivatives in a property-sheet mode of the DPF operation obtained at all 4 PSSs

Maximal current amplitude was detected with 4 capacitors (with the whole bank) at

Notes:

1. The current derivative trace is dI/dt taken at one of the 4 PSSs.

2. Inductance (static) of bank L_0 is not given; we will fit it unambiguously from the slope of the computed current trace fitted to the measured current.

3. Stray resistance of bank is not given; we will use 0.1 of surge impedance of bank and check that this is consistent during the fitting.

4. We only have the waveform; ie the shape of the current trace taken at one of the 4 PSSs. However the model code we are using is charge-‘consistent. Hence once we have the current waveform correctly fitted, the computed current amplitudes are correct and may be used to calibrate the system current; we assume the shape of the current trace at the PSS that we are using is consistent with the overall current waveform.

Data treatment

- **Tracing the dI/dt, filtering out the high frequency 'noise' oscillations**
- Since we have no digital file, we trace out the dI/dt **Current derivative trace; (from pg 84 Fig 89 bottom-most trace)** as best we could (filtering out the high frequency 'noise' oscillations by drawing a line through the middle of the high frequency 'noise' oscillations as judged visually. We obtained the following as shown in Figure 2.1 after an inversion to obtain the starting dI/dt positive.

Extracted dI/dt

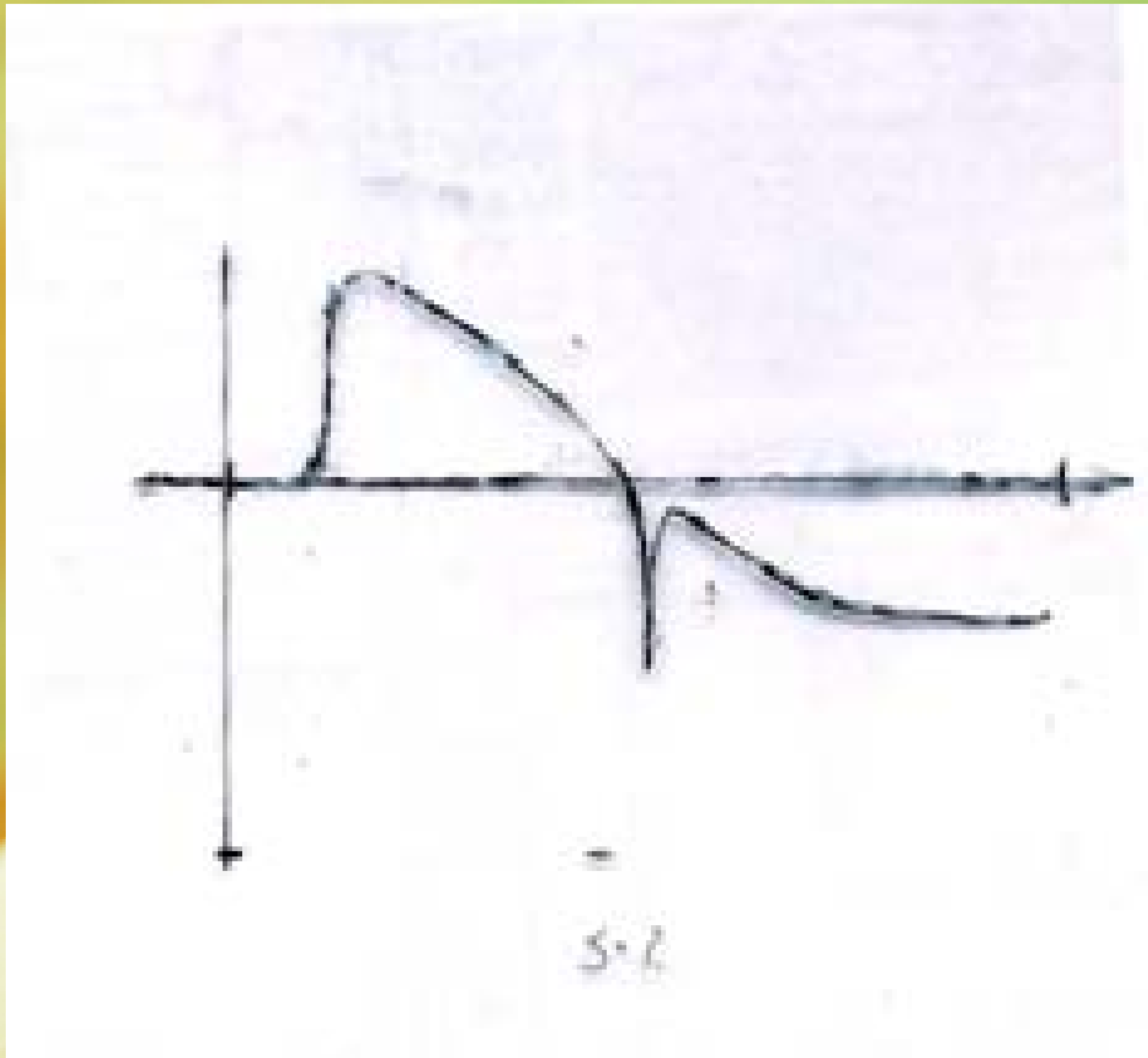

Converting extracted image to digital file

Then we digitized this trace using a digitizer called “Engauge” obtaining the digitize
trace & its integration is shown in Figure 2.2 (a screen capture).

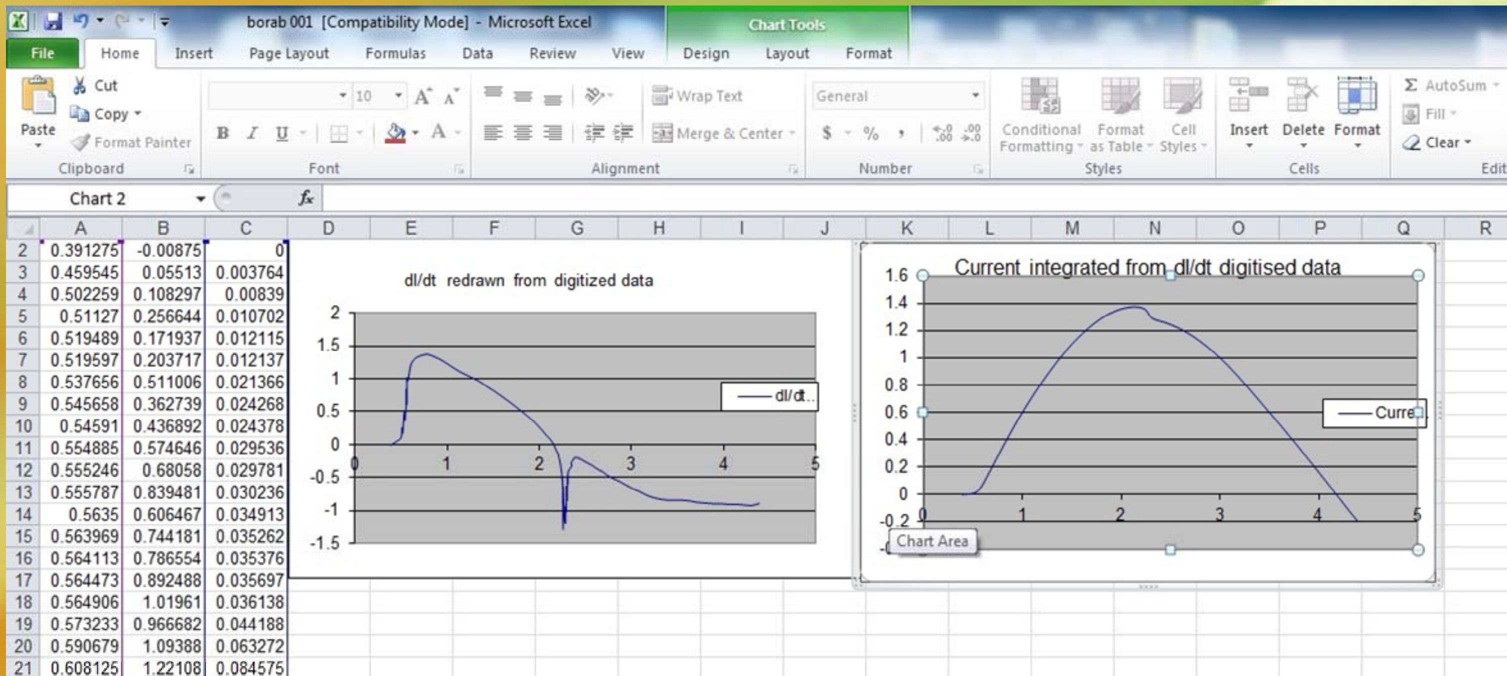

	A	B	C
2	0.391275	-0.00875	0
3	0.459545	0.05513	0.003764
4	0.502259	0.108297	0.00839
5	0.51127	0.256644	0.010702
6	0.519489	0.171937	0.012115
7	0.519597	0.203717	0.012137
8	0.537656	0.511006	0.021366
9	0.545658	0.362739	0.024268
10	0.54591	0.436892	0.024378
11	0.554885	0.574646	0.029536
12	0.555246	0.68058	0.029781
13	0.555787	0.839481	0.030236
14	0.5635	0.606467	0.034913
15	0.563969	0.744181	0.035262
16	0.564113	0.786554	0.035376
17	0.564473	0.892488	0.035697
18	0.564906	1.01961	0.036138
19	0.573233	0.966682	0.044188
20	0.590679	1.09388	0.063272
21	0.608125	1.22108	0.084575

Figure 2.2 Digitized dI/dt trace and the integrated measured current waveform

Using the measured current trace for fittings of the computed current trace to 'calibrate' the model code to the Bora Plasma Focus

We configure the UPFL (**RADPFV5.15df.xls**) for Bora using the following trial configuration.

Values in black: given; **Values in red: trial**

Lo nH	Co uF	b cm	a cm	zo cm	ro mΩ
30	24.4	2.5	1.5	4	2.3
massf	currf	massfr	currfr	Model Parameters	
0.07	0.7	0.16	0.7		

Vo kV	Po Torr	MW	A	At=1 mol=2	Operational Parameters
17	7.6	4	1	2	

- In order to make the comparison meaningful we note:

- The computed curve and the measured curve may need to be shifted in time one relative to the other. To do that we add an amount of time (time shift) specified in Cell K1 which is varied until the start of the computed and measured traces coincide.
- The measured current has unknown (hence treated as arbitrary) amplitude. To make meaningful fit it is necessary to adjust the measured current amplitude to that of the computed amplitude. To do this we place a multiplying factor (multiplier) in Cell L1 which is varied until the measured amplitude is equal to the computed. Then we start the profile (shape) fitting.

Fitting the static inductance L_0.

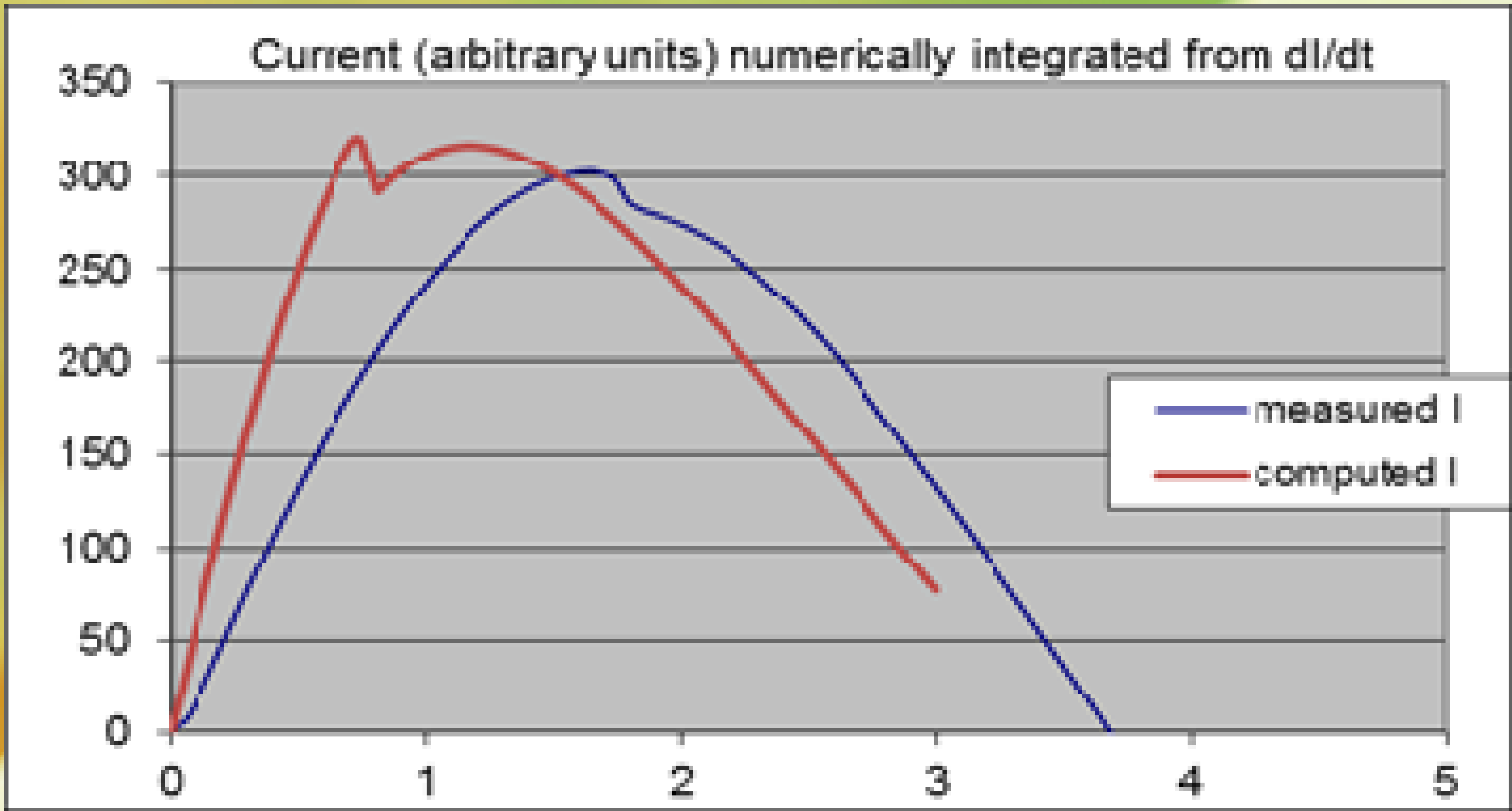

- Then fit fm, fc
- Then fit fmr, fcr
- Also fit ro

Final fitted configuration

Lo	Co	b	a	zo	ro mOhm	
55	24.4	2.5	1.5	6	6	
massf	currf	massfr	currfr	Model Parameters		
0.2	0.7	0.4	0.7			
Vo	Po	MW	A	At-1 mol-2		Operatio
17	7.6	4	1	2		Paramet

Final fit is good

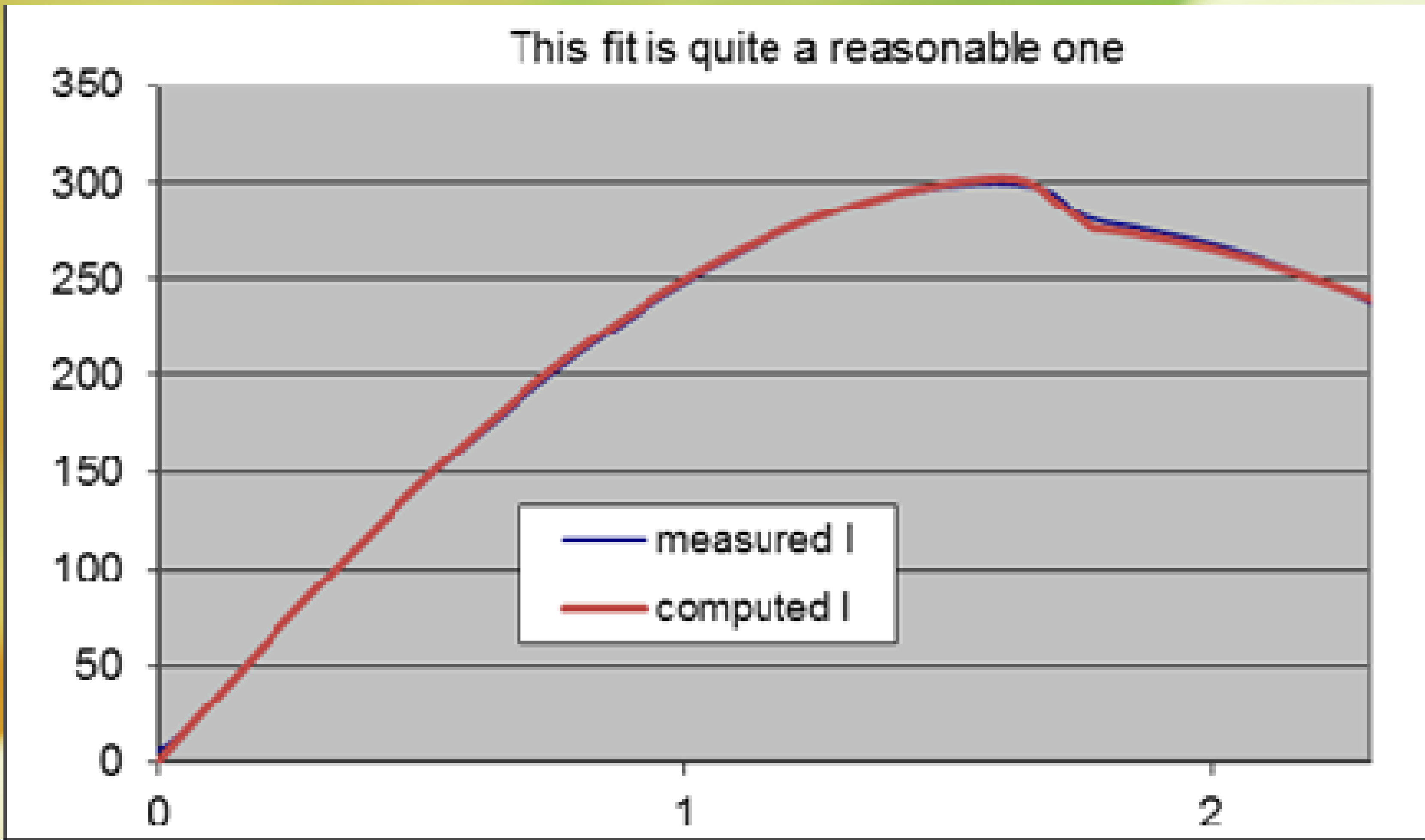

7 Concluding Notes

The inductance (55 nH fitted) is surprisingly high when compared with the predecessors PF-5M (33 nH) or NX1 (30 nH). The Designer of BORA will be able to confirm this aspect of the design in comparing with PF-5M and NX1.

2. The mass factor f_m and radial mass factor f_{mr} are unusually high indicating (a) that the solid channel of the Bora is conducive to a more efficient mass swept-up (b) and the possibility that the pressure that was actually in the chamber could be higher than "about" 10 mbar as stated against Fig 89;

Peak circuit current Ipeak=304 kA and
the neutron yield Yn= $1.9\text{x}10^8$.

The dynamics and some Pinch Properties are presented in the following screen capturein the next page.

Once fitted, the dynamics, plasma dimensions and plasma temperature and density are all outputt the code

- Note that our input is just this:

The final conditioning of the device has resulted in its proper operation at 17-18 kV with deuterium pressure of about 10 mbar. Corresponding oscilloscope traces obtained by miniature magnetic probes installed near each of our 4 PSSs are presented in Fig. 89.

From this picture one may see that the rise-time of current of our main discharge is equal to about 1.5 μs with the "peculiarity" of the current positioned in a proper place at the moment of 1.8 microsecond from the start of the discharge. By means of Rogowski coil we have measured the amplitude of our discharge current. With 3 capacitors and maximal achievable voltage (19.5 kV) supplied by our charger we obtained the current magnitude equal to 234 kA.

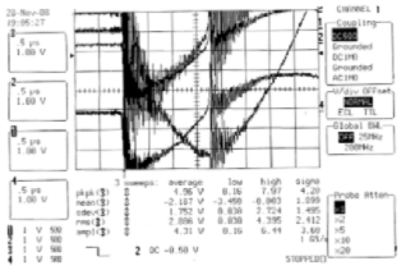

Fig. 89 Oscilloscope traces of the discharge current derivatives in a property sheet mode of the DPF operation obtained at all 4 PSSs

Maximal current amplitude was detected with 4 capacitors (with the whole bank) at 18 kV of charging voltage and with initial deuterium pressure of 11 mbar. It was equal to about I_{SF} = 300 kA. With this current, according to a well-known experimental scaling law for neutron production by DPF with deuterium as a working gas, we may expect neutron yield in a single shot on the level of:

$$Y_n \approx 10^{10} \times I_{SF}^4 \approx 10^{10} \times (0.3)^4 \approx 10^8 \text{ neutrons/pulse} \quad (12)$$

Hands-on numerical experiment will be carried out in the next two hours